A comparative and parametric study of experimentally obtained flutter derivatives of four bridge decks – streamlined and bluff shapes

by

John Michael Stronck

A thesis submitted to the graduate faculty

in partial fulfillment of the requirements for the degree of

MASTER OF SCIENCE

Major: Aerospace Engineering

Program of Study Committee:
Partha P. Sarkar, Major Professor
Fred Haan
Mani Mina

Iowa State University
Ames, Iowa
2005

Graduate College
Iowa State University

This is to certify that the master's thesis of

John Michael Stronck

has met the thesis requirements of Iowa State University

Signatures have been redacted for privacy

Dedication

I would like to dedicate this work to William (Bill) L. Rickard. Had it not been for his confidence in my character my association with the Iowa State University Wind Simulation and Testing Laboratory as well as the Iowa State University faculty would have been very limited. I thank him for the years of guidance, teaching, sharing of ideas, and, most importantly his friendship.

I want to especially thank my girlfriend, Melanie, for her perseverance in keeping me sane and happy throughout my trials and tribulations with my research. She has been a great inspiration to my work ethic and maintaining a kind personality in times of great stress.

Table of Contents

List of Tables

List of Figures

Abstract

Flutter instability is of major concern for the design of flexible structures such as long span bridges and airplane wings. Flutter analysis of structures is usually done in frequency domain. Alternately, time-domain methods have been suggested. Both approaches require the identification of aeroelastic parameters such as flutter derivatives in frequency domain and Rational Function Coefficients or Indicial Functions in time domain. Flutter derivatives that are used for flutter analysis can be identified from section model testing in a wind tunnel. The art of efficient extraction of these aeroelastic parameters requires an elastic suspension system to capture coupled displacement and aerodynamic force time histories from wind tunnel testing of section models. A variety of methods have been employed to extract flutter derivatives including free-vibration, forced-oscillation, and computational fluid dynamics.

A recent technique developed at the Iowa State University Wind Simulation and Testing Laboratory (ISU WiST Lab) utilizes a three degree-of-freedom (DOF) free-vibration suspension system for data acquisition and recently developed system identification software (Iterative least squares method or ILS method) for data analysis. Testing the robustness of this technique was critical for establishing confidence in the obtained flutter derivatives. Another important aspect of wind tunnel testing is the ability to develop realistic models capable of providing means to obtain reliable pressure and /or force data while maintaining rigidity and minimal weight.

The main purpose of this research was to scrutinize the free-vibration technique used in the ISU WiST Lab to offer improvements to the system and techniques used for data acquisition and analysis and to contribute new model building methods for future testing. The system verification involved design and construction of bridge deck section models,

acquiring displacement time histories from wind tunnel testing, analyzing the acquired data with an improved version of the ILS System ID software, and finally comparing obtained flutter derivatives with those from other sources.

The parametric study involved comparing flutter derivative data between stable and unstable bridge decks, longer and shorter section model lengths, and solid-streamlined versus slotted-streamlined bridge decks. These studies helped to illustrate the importance of bridge cross sectional shapes for aerodynamic stability and model design and construction for proper testing. For the comparative study, bridge models were tested in two separate single DOF cases (vertical and then torsional) and a two DOF case (vertical and torsional). The direct flutter derivatives were compared between the single DOF cases and the two DOF case as well as with data from outside sources to establish further confidence in system operation.

Chapter 1: Introduction

1.1 Objectives and Motivation

The evolution of wind engineering took place over many centuries during which it has seen many wind-related disasters that helped its cause. Although the term "wind engineering" was not implemented until 1970, many pioneers had already developed the fundamentals of today's wind engineering study in the centuries prior to the time when the study received the current nomenclature. Some of the pioneers of wind engineering and their findings included Newton's definition of viscosity and laws of motion as formulated in the late 1600's, Euler's formulation of equations defining inviscid fluid motion in 1755, Prandtl's development of the boundary-layer concept in 1904, and von Kármán's identification of vortex shedding in wakes in 1912. During the development of wind engineering, many wind-related disasters on structures occurred. Disasters to bridge structures due to wind include Scotland's Tay Bridge in 1879 and the Tacoma Narrows Bridge in 1940 (Cochran [1]). Figure (1) shows the Tacoma Narrows Bridge just before collapse due to wind-induced vibration at a wind speed of 42 mph.

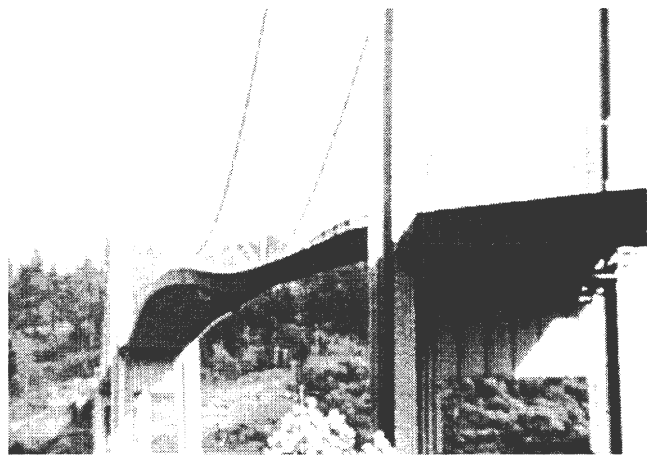

Figure 1. Collapse of Tacoma Narrows Bridge Deck (Photo courtesy of University of Washington Libraries)

The ISU Wind Simulation and Testing Laboratory (WiST Lab) has developed a system utilizing section models to study aeroelastic phenomena of a variety of aerodynamic configurations. These aerodynamic configurations can consist of bridge decks, aircraft components, or any other structures affected by aerodynamic forces. This system consists of section models suspended in a three degree of freedom (DOF) suspension system allowing the models to move freely when subjected to wind loading. Although the suspension system was designed with the capability to test models with motions in all three degrees of freedom (vertical, lateral, and torsional), this study involves fixing the lateral motion allowing only two degrees of freedom in the torsional and vertical directions. The objectives of this research were to perform a comparative and parametric study of bridge decks of various shapes, using section models, to check the robustness of the suspension system, develop more easily executable methods of operation of the suspension system, incorporate different model-building techniques depending on the type of data taken and the complexity of the section model, and develop the flutter derivative extraction software into a more user-friendly version. With these improvements, bridge deck flutter analysis in the ISU WiST Lab could be more efficiently executed with increased confidence in the output data. A more efficient executability and output-data confidence would allow more extensive use of the free-vibration and forced-oscillation systems for testing and understanding the response of a variety of section models. These tests would help to ensure the proper design of bridge decks and other structures, so as to provide safer and more stable structures.

The method used for checking the robustness of the system involved testing a variety of models representing streamlined and bluff shapes that were predetermined as stable or unstable. This data was then compared to output data obtained from other tests in the WiST

Lab and other institutions where different flutter derivative extraction techniques were used. The parametric study included modification of section models for further testing to reveal the effects of these modifications as well as modification of the test parameters on the final output, i.e. flutter derivatives. The modifications of the suspension system involved a change in the measurement and release technique for initial conditions as well as adjustments to the suspension system and the models placed on the suspension system. New model construction techniques had to be implemented due to complex model configurations, type of data acquisition being utilized, and for ease of model construction. Design criteria were also addressed during the design and construction of the models using the newly implemented construction techniques. The initial flutter derivative extraction software developed at the ISU WiST Lab [1] was designed to be application specific. Since multiple models had to be tested, this software needed to be upgraded for easy usage regardless of the test parameters. Together, all of these changes helped to create a more robust system, not only in the data acquisition stage, but also during the data analysis and processing stage. The most important purpose of this research was to instill more confidence in the free vibration flutter derivative analysis technique used in the ISU WiST Lab.

1.2 Aeroelasticity and Flutter Phenomenon

The collapse of the Tacoma Narrows Bridge initiated a greater scrutiny in the wind engineering discipline of aeroelasticity. Aeroelasticity involves the study of the interaction of aerodynamic forces with structural motions. Bridges and other large structures require careful consideration of "aeroelastic" effects due to dynamic wind loading. As a bridge is subjected to wind loading, the relative orientation of the structure with respect to the flow can

change causing the aerodynamic loads on the structure to change. Similarly, a shift in wind direction with respect to the structure can produce different aerodynamic loads since the structure would project a different cross section with respect to the wind direction. This dynamic and often complex interaction of the wind with the structure can lead to a monotonically increasing response once the wind speeds reach a critical value. This phenomenon, in which a flexible structure looses its ability to resist the aerodynamic loads due to loss of its mechanical damping or stiffness leading to growing oscillations, is known as flutter. The failure of the Tacoma Narrows Bridge was due to a combination of steady and unsteady wind loading causing a self-excited oscillation of the bridge structure and eventually leading to the destruction of the bridge. If a structure cannot be made rigid enough to prevent oscillatory motion due to wind loading, then the next consideration would be to develop a cross section that has greater stability characteristics in wind. The flutter susceptibility of a structure can be predicted by a set of parameters called flutter derivatives. Flutter derivatives quantitatively describe the aeroelastic forces. These parameters can be extracted by testing geometrically scaled models in wind tunnels.

1.3 Current Work

The primary tasks in this work were to further develop the free-vibration and forced-oscillation systems, used for flutter derivative extraction, into more efficient and dependable devices. Current work includes construction of additional section models using a rapid prototyping approach. Using rapid prototyping to construct future section models will help to incorporate pressure taps in models with complex geometries. This approach to model design and construction will be discussed more thoroughly later in the paper. A forced-

oscillation system was in the final development stages at the time of writing this thesis. This system utilizes the same test section in which the free-vibration system was built making the conversion of the free-vibration system to this system relatively simple.

1.4 Organization of this Study

This thesis illustrates the free-vibration setup and its operation and mentions the improvements performed on the ISU WiST Lab free-vibration suspension system and the flutter derivative extraction method that is used in conjunction with the free-vibration system. Chapter 2 gives an overview of different flutter derivative extraction methods. A detailed discussion of the free-vibration flutter derivative extraction technique is provided. It also provides the background on the free-vibration flutter derivative extraction technique used in the ISU WiST Lab, including construction of the test setup and the initial development of the analysis software. Chapter 3 discusses the current experimental procedure as well as model preparation techniques. This will involve an explanation on wind tunnel model construction and design, wind tunnel model and test section preparation, data acquisition procedures, and System Identification Code improvement. It also illustrates flutter derivative comparison methods used to verify proper operation of the ISU WiST Lab system. Chapter 4 discusses some comparisons made between different types of bridge deck models. This includes a study of bridge decks that are bluff-shaped versus streamlined, streamlined box girder versus slotted-streamlined box girder, and aerodynamically unstable versus aerodynamically stable. The effects of section model lengths and initial displacements used during testing were studied and discussed here. The aforementioned studies prove the importance of model design and the meticulous nature of the free-vibration testing method. Chapter 5 gives a summary of all results and modifications that were performed with the free-vibration

suspension system and with the system identification software including conclusions for the section model testing and design. This final chapter also mentions further recommendations and future research that can be performed with this system as well as with the forced-oscillation system.

Chapter 2: Background

2.1 Equations of Motion

The free-vibration method for the extraction of flutter derivatives uses displacement response time histories of a section model that oscillates at a certain wind speed inside a wind tunnel. The displacement time histories capture the effects of aeroelastic forces on the oscillation frequency and damping of the rigid model. Flutter analysis that results in prediction of flutter speed and flutter frequency is accomplished by applying these experimentally acquired flutter derivatives towards the real world structures that the models represent. This research involved the extraction of up to eight flutter derivatives for each section model using either a single or two degree of freedom (DOF) system. The three-DOF suspension system used for this research has the ability of allowing different combinations of degrees of freedom, whether single-DOF, two-DOF, or three-DOF. The eight flutter derivatives that were extracted are associated with the torsional and vertical degrees of freedom. Figure (2) shows the defined degrees of freedom used for this research project.

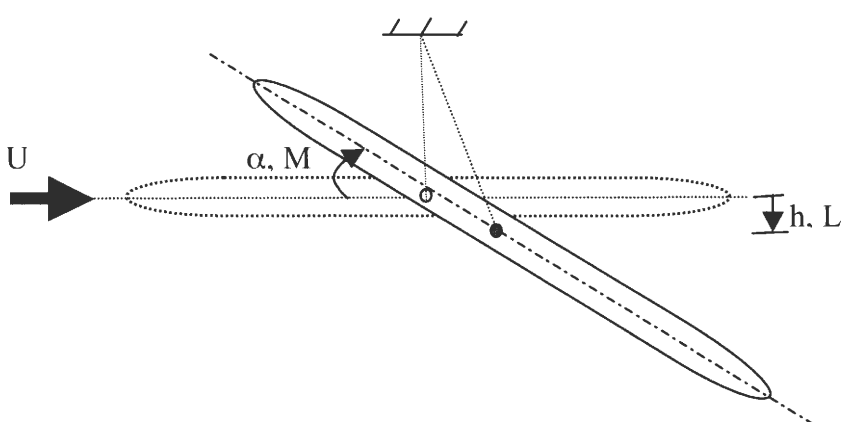

Figure 2. Illustration of degrees of freedom used for section model testing

In the two-DOF model illustrated in Figure (2), α is the torsional deflection and h is the vertical deflection. Aerodynamic forces acting on the section model are lift (L) and moment (M). Section model properties are m_h and I_α defined as vertically oscillating mass per unit length and moment of inertia per unit length, respectively. Other section model properties include the mechanical damping ratios ζ_h and ζ_α as well as the natural mechanical frequencies ω_h and ω_α for vertical and torsional motion, respectively. Chowdhury and Sarkar [3] explain the setup of the system identification method used for the flutter derivative extraction for a three-DOF free-vibration system. The three-DOF setup produces 18 flutter derivatives. Since this research only explores the two-DOF case, only eight flutter derivatives will result from the analysis. Equation (1) is the equation of motion used to describe the free-vibration oscillation of the section model.

$$\underline{\ddot{y}} + \underline{M}^{-1}\underline{C}\underline{\dot{y}} + \underline{M}^{-1}\underline{K}\underline{y} = \underline{M}^{-1}\underline{F}_{ae} \tag{1}$$

In Equation (1),

$$\underline{y} = \{h \quad \alpha\}^T,$$

$$\underline{M} = \begin{bmatrix} m_h & 0 \\ 0 & I_\alpha \end{bmatrix}, \quad \underline{M}^{-1}\underline{C} = \begin{bmatrix} 2\varsigma_h\omega_h & 0 \\ 0 & 2\varsigma_h\omega_h \end{bmatrix}, \quad \underline{M}^{-1}\underline{K} = \begin{bmatrix} \omega_h^2 & 0 \\ 0 & \omega_\alpha^2 \end{bmatrix}.$$

Equation (2) shows how the aeroelastic force vector is formed.

$$\underline{F}_{ae} = \begin{Bmatrix} L_{ae} \\ M_{ae} \end{Bmatrix} = \begin{bmatrix} 0.5\rho\, U^2 B & 0 \\ 0 & 0.5\rho\, U^2 B^2 \end{bmatrix} \cdot$$

$$\cdot \begin{bmatrix} KH_1^*/U & KH_2^* B/U & K^2 H_4^*/B & K^2 H_3^* \\ KA_1^*/U & KA_2^* B/U & K^2 A_4^*/B & K^2 A_3^* \end{bmatrix} \begin{Bmatrix} \dot{h} \\ \dot{\alpha} \\ h \\ \alpha \end{Bmatrix} \tag{2}$$

In Equation (2), ρ is the air density; U is the test section mean wind velocity; K is the non-dimensional reduced frequency, $K=B\omega / U$; and ω is the angular frequency of oscillation. The non-dimensional aerodynamic coefficients from Equation (2) H_i^* and A_i^* (i = 1, 2, 3, 4) are called the flutter derivatives. Chowdhury and Sarkar [3] have derived the expressions solving for the flutter derivatives using the elements of the stiffness and damping matrices associated with each flutter derivative.

Earlier it was mentioned that the three-DOF system could be configured so to allow for movement in any combination of degrees of freedom. For this research the combinations included a vertical single-DOF, torsional single-DOF, and two-DOF (vertical and torsional). The flutter derivatives obtained from the vertical single-DOF case included H_1^* and H_4^*. These flutter derivatives are known as the vertical direct flutter derivatives. The torsional single-DOF case provides the flutter derivatives A_2^* and A_3^*, also known as the torsional direct flutter derivatives. The direct flutter derivatives from the single-DOF cases are compared to the direct flutter derivatives from the two-DOF case for a given section model. These terms are known as direct flutter derivatives since they directly relate to the DOF with which they are associated. The vertical direct flutter derivative H_1^* is associated with vertical

velocity and influences the vertical damping. The vertical direct flutter derivative H_4^* is associated with vertical displacement and influences the vertical stiffness. The torsional direct flutter derivative A_2^* is associated with the angular velocity and influences torsional damping, while the torsional direct flutter derivative A_3^* is associated with the angular displacement and influences torsional stiffness.

2.2 Flutter Derivative Extraction Techniques

There exists a variety of methods to perform experimental and computational flutter derivative extraction. A comparison of flutter derivatives obtained from different methods can suggest the relative accuracy of each method. As mentioned earlier, one particular example of a flutter derivative extraction technique involves the use of a free-vibration suspension system. All the data for this research was obtained using this type of system, so it is described in detail later. Another technique involves the use of a forced-oscillation suspension system. A description of the system designed and fabricated for the Bill James Wind Tunnel of the WiST Lab and integrated with the free-vibration system is also provided. A brief explanation of the use of computational fluid dynamics (CFD) for the extraction of flutter derivatives will be the final part of the discussion among the methods used.

Free-Vibration Method

As mentioned earlier, the free-vibration method for flutter derivative extraction involves the use of a three-DOF suspension system to allow free movement of a section model in all three degrees of freedom. These degrees of freedom as available for the suspension system inside the test section of the ISU WiST Lab Bill James Wind Tunnel consist of vertical or galloping motion, lateral motion, and a pitching or torsional motion.

For this research, the free-vibration system was used in the two-DOF mode consisting of vertical and torsional motions (lateral motion is arrested), single degree of freedom (SDOF) vertical mode, and a SDOF torsional mode. In this method, the model is subjected to initial displacements and its free-vibration motions are recorded at a particular wind speed before increasing the speed to the next level. The procedure is repeated until a preselected range of reduced velocities is covered.

Equation (3) is used to identify the reduced velocity for a given wind speed, model width (measured along the wind direction), and frequency of model oscillation.

$$V = \frac{U}{nB} \tag{3}$$

In the reduced velocity equation, V is the reduced velocity; U is the wind speed in the wind tunnel test section; n is the angular frequency of oscillation, $n=\omega/2\pi$; and B is the width of the section model. The reduced velocity is a parameter used to compare similar shaped models of different sizes and natural frequencies.

The system utilizes an arrangement of force transducers that are used to measure the loads transmitted through linear springs. These loads can be converted to model displacements using the known spring stiffnesses. The displacement time histories, as recorded, are used to identify the damping and frequency characteristics of the section model utilizing a system identification method. These damping and frequency characteristics define the flutter derivatives for that particular cross section. Figure (3) illustrates the layout of the ISU WiST Lab free-vibration suspension system test section.

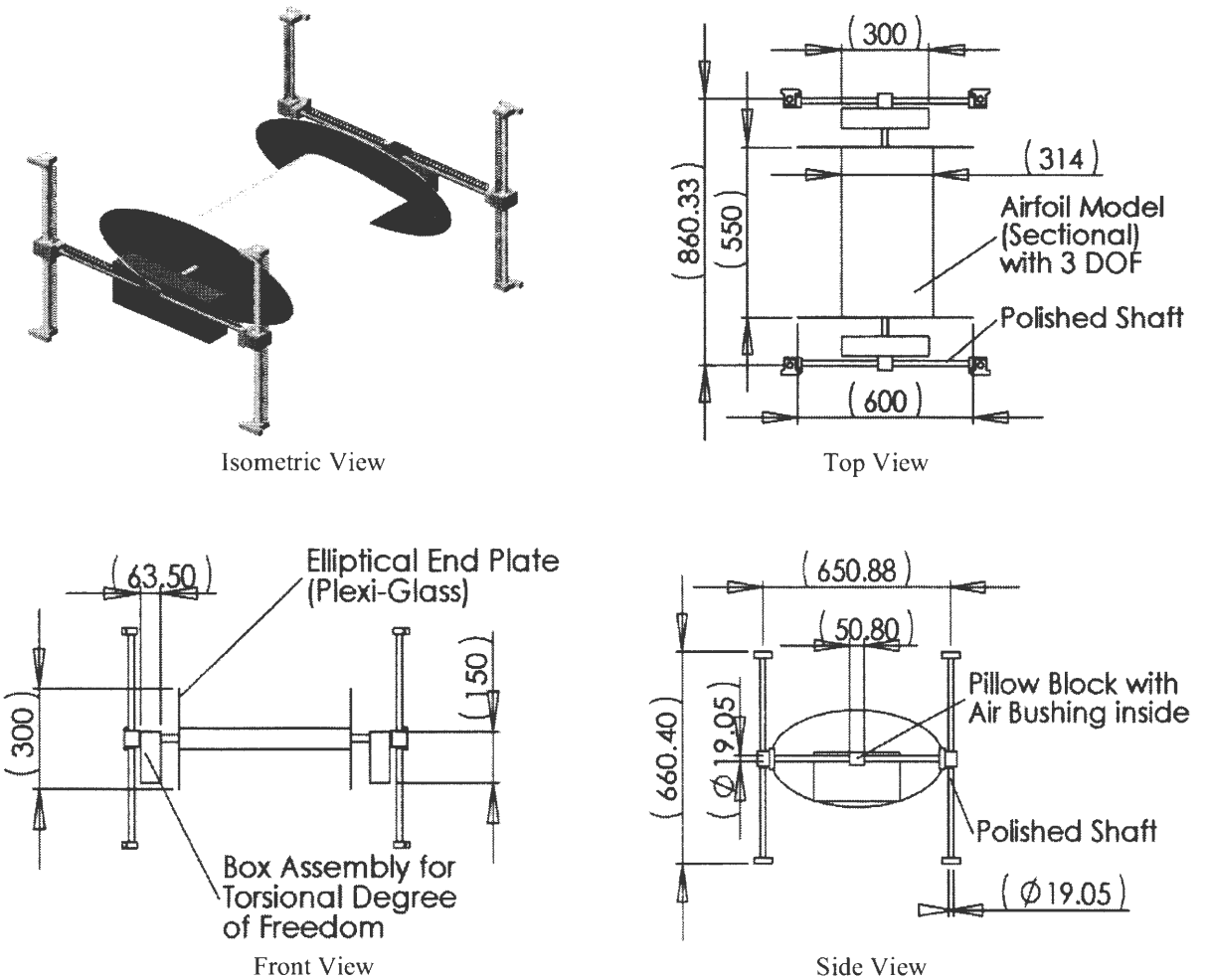

Figure 3. Three-DOF suspension system layout (Diagrams courtesy of Chowdhury)

Forced-Oscillation System

As stated earlier, the forced-oscillation system was developed utilizing the same test setup as the free-vibration system in the Bill James Wind Tunnel. Instead of allowing the model to vibrate freely, as in the free-vibration method, the forced-oscillation method involves oscillating the model in SDOF or two-DOF motions at fixed frequencies at a fixed wind speed. As the model oscillates, pressures are recorded along the surfaces of the model. Simultaneously, the time histories of the model motions are recorded.

In this method, the model is subjected to either vertical or torsional SDOF motion and pressures are recorded with the aid of two 16-channel Scanivalve pressure transducers. One pressure transducer records pressures at taps located along the bottom of the section model, while the other records pressures at taps along the top of the model. The phase difference between the model displacement time history and the pressure distribution or aeroelastic force time history is an important variable for extracting the flutter derivatives using the forced-oscillation approach. With the forced-oscillation method, the reduced velocity for a particular test can be altered either by changing the frequency of oscillation or the wind speed in the test section. In contrast, increasing the wind speed in the test section is the only direct approach for changing the reduced velocity for the free-vibration method.

Figures (4) and (5) show the Bill James Wind Tunnel free-vibration test section converted into a forced-oscillation system. Figure (4) shows the overall configuration of the forced-oscillation system, while Figure (5) specifically illustrates how the forced-oscillation system is incorporated into the free-vibration suspension system. An externally-mounted pseudo-bridge-deck actuates the section model via pushrods. Initial tests to check performance of the forced-oscillation system were conducted using a section model previously tested with the free-vibration system. The purpose of this testing was for establishing operating procedures, cross checking flutter derivatives obtained with the free-vibration method, and to make adjustments to the forced-oscillation system. Preliminary results of flutter derivatives that were extracted using this method are not reported here because this was outside the original scope of this research.

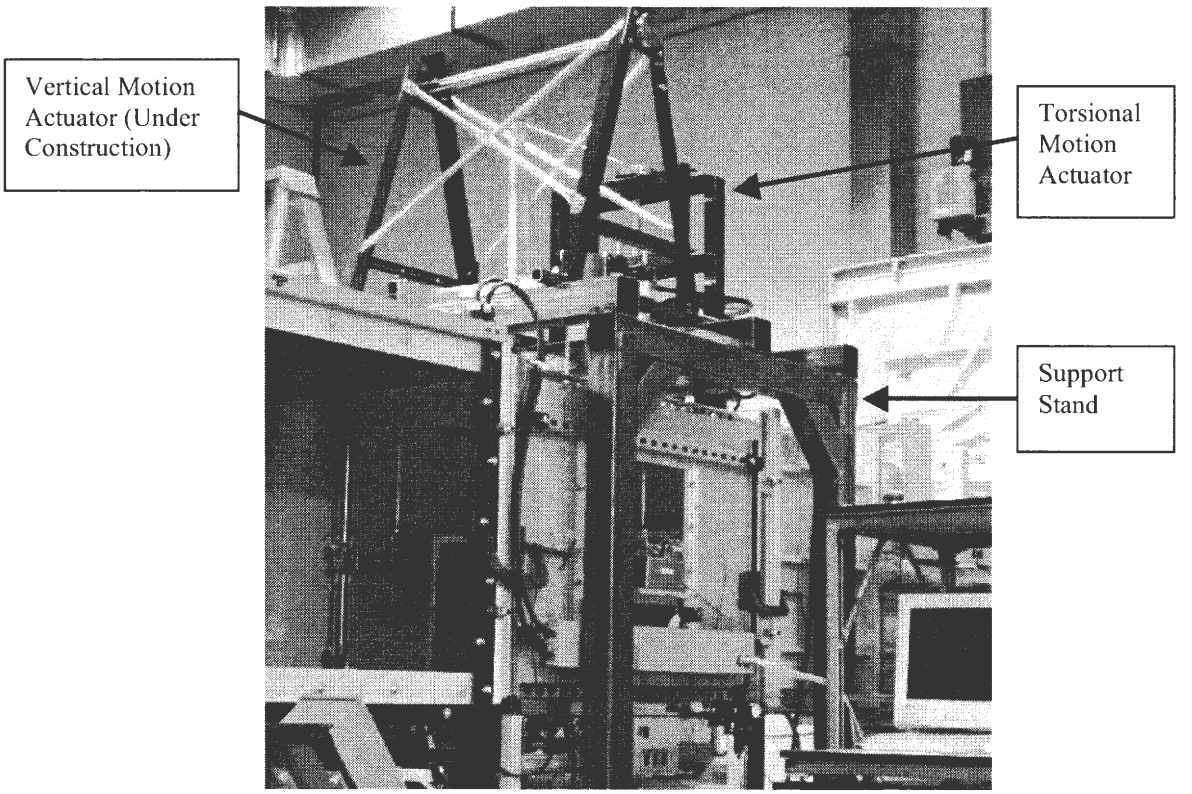

Figure 4. External view of Bill James Wind Tunnel forced-oscillation system

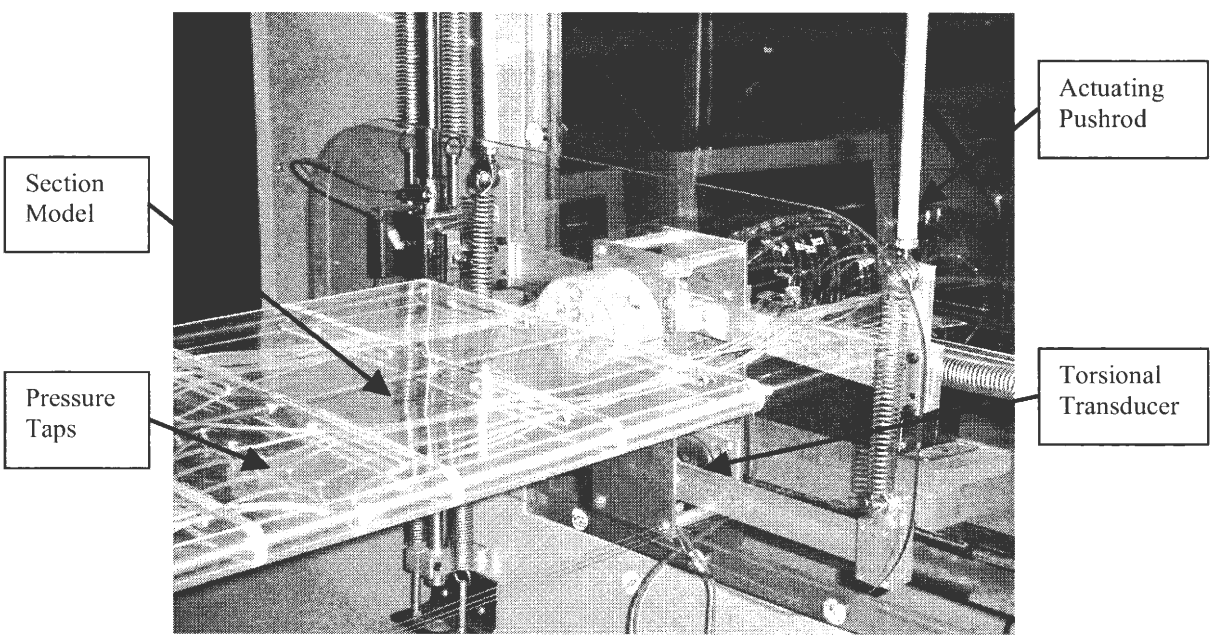

Figure 5. View showing the forced-oscillation system with a model inside the test section

Computational Fluid Dynamics (CFD) Approach

Another method used to extract flutter derivatives is by use of CFD. Although CFD has not been used in this study in conjunction with the experimental work, it is worth mentioning it here. Some benefits of using CFD are that it does not require the use of a wind tunnel, section models, or data acquisition equipment. These components can be very expensive and require much attention and time for proper set up, design, and operation. Some drawbacks of CFD are the use of extensive and expensive computer systems capable of supporting the amount of calculations involved in the complex analysis of flutter, although more recent computer advances have allowed higher computing power at reasonable costs. Further, accuracy is always an issue in CFD output, more so than experimental results. Several methods, such as Discrete Vortex Simulation (DVS), Finite Element Method (FEM), and Large Eddy Simulation (LES) have been employed to analyze aeroelastic behavior with the CFD approach. Braun and Awruch's [4] review of CFD approaches explains that one of the first publishers of a CFD method for analyzing aeroelastic phenomenon was Kawahara and Hirano in 1983. In this study, Kawahara and Hirano used FEM to obtain the Strouhal number and the aerodynamic coefficients as functions of angle of attack.

Larsen and Walther [5] analyzed five generic bridge decks in 1997 to test a discrete vortex method (DVM) for computational extraction of aerodynamic parameters of two-dimensional (2D) bluff cross-sections. Their analyses yielded root mean square lift coefficients and Strouhal numbers for static cross sections. The dynamic analysis resulted in flutter derivatives for the bridge deck cross sections undergoing a forced galloping and twisting motion. A DVM code called DVMFLOW was used to create a 2D viscous simulation of the vorticity equation. Larsen and Walther make a reference to the

mathematical model for vorticity. The DVMFLOW code input consists of a boundary panel model of the bridge deck contour. Output consists of time progressive simulations of surface pressures and section loads. The induced velocity field and vortex positions are mapped as part of the output. Aerodynamic derivatives are obtained through post processing of the simulated time histories. Most CFD approaches to flutter derivative extraction are accomplished with similar techniques.

Comparison of Free-Vibration versus Forced-Oscillation

Although the free-vibration and forced-oscillation approaches use the same test section in the ISU WiST Lab Bill James Wind Tunnel, there are many differences between the operation and characteristics of each system. The free-vibration method allows the section model to move in a natural state. This allows an examination of the behavior of the bridge deck in a self-excited state. But if an unstable model is tested without proper supervision, the model can oscillate violently causing damage to the suspension system or the model. Since the forced-oscillation method involves driving the rigid model with a robust drive system, the model does not experience any motion caused by the wind in the test section. This also prevents the model from experiencing violent oscillatory behavior.

As stated in the sections describing the forced-oscillation and free vibration systems, the two systems utilize different methods to obtain and analyze data. The free-vibration system uses force transducers to take data that is later converted into displacements. During testing, the free-vibration data acquisition method appeared less faulty and more robust. The force transducers have the ability to take data at the smallest of oscillation amplitudes and at any combination of wind speed and section model configuration. On the other hand, the pressure transducers used for the forced-oscillation system were usually difficult to

communicate with and configure. Other problems with the forced-oscillation system arise when wind tunnel velocities are below or above certain magnitudes. When velocities are low, pressures recorded by the pressure transducers are hard to distinguish from noise. When velocities are high, the pressure transducers have the chance of becoming saturated.

The physical operation of the forced-oscillation system is more easily executed than the initiation of the operation for the free-vibration system. The free-vibration system uses strings attached to the section model to force the model to an initial displacement. These strings are held by electromagnets for simultaneous release of all strings. At greater initial amplitudes and wind speeds, some strings don't release properly causing an erratic motion in the section model. Setting the initial displacements to magnitudes that allow an error-free release can be tedious. With the forced-oscillation system, the initial amplitude is already fixed by the amount of travel allowed in the actuator. For the forced-oscillation system, the model is in constant motion. This allows many tests to be taken at the same test settings without the need to restart the oscillations between each data series.

2.3 Parametric Dependencies of Flutter Derivatives

Wind tunnel aeroelastic measurements and analyses require careful planning and stringent testing methods and procedures. Variations in the airflow whether smooth or turbulent, the orientation of the section model with respect to the mean flow also known as angle of attack, the type of model and dimensions of the model, and frequency and initial amplitude of oscillation affect the outcome of the flutter derivatives. These variations can cause the section model to behave differently from what is expected.

Smooth versus Turbulent Flow

Flow regimes can completely skew the outcome of a particular section model from the expected outcome. A study performed by Ming Gu and Xian-Rong Qin [6] entertained the difference in flutter derivatives in a turbulent flow as opposed to a smooth flow. These studies were performed on a streamlined bridge deck section model and a section model of the Hong-Guang Bridge located in southwestern China. The Hong-Guang Bridge is a cable-supported bridge of blunt Π type with a main span of 380m. The study involved a numerical simulation as well as an experimental test of each model for comparative analysis.

Although the turbulent scales used in this study were of smaller magnitudes than those experienced in the atmosphere, this study gives a reasonable idea of the conditions caused by dynamic flow regimes. According to Gu and Qin, flutter derivatives corresponding to aerodynamic stiffness, H_3^* and A_3^*, have negligible changes when subjected to either smooth flow or turbulent flow. However, flutter derivatives corresponding to aerodynamic damping for the Hong-Guang Bridge deck, specifically H_2^*, A_1^*, and A_2^*, confirm a prominent deviation from the equivalent flutter derivatives in smooth flow. This study would suggest that blunt aerodynamic bodies, especially the Π-type section, should be analyzed in a turbulent flow as well as a smooth flow. The damping response of the model is important to stability. When the type of flow has significant effects on the response of the model, it should be subjected to turbulent flow to verify that the model would still behave properly with the different flow conditions.

Effects of Amplitude, Frequency, and Angle of Attack

Testing parameters can have a significant influence on the data obtained from section model testing. For instance, damping is dependant on amplitude. With this concept in mind,

careful consideration must be given to starting amplitudes for free-vibration flutter derivative extraction. Since a free-vibration system allows free movement of the section model, higher starting amplitudes can result in a response with greater initial damping. Consequently, careful adjustment of the initial amplitude must be considered during free-vibration testing to obtain congruent output data.

The frequency of oscillation of the section model plays an important role in experimental planning for flutter analysis. According to Equation (3), the reduced velocity is dependent on the angular frequency of oscillation. To allow flutter analysis in the reduced velocity range selected, careful attention must be paid to the natural frequency of the system and the range of wind speeds that can be generated in the wind tunnel as well as other considerations. The natural frequency of the system depends on the mass of parts of the suspension system, including the model, in motion for the selected degree-of-freedom as well as the stiffness of the springs in the suspension system. Adjusting the mass of the system is somewhat easier for making small adjustments in the natural frequency, since changing of springs requires partial disassembly of the suspension system. However, changing of the springs with a specific stiffness is required to make large and gross adjustments of the natural frequency.

Proper selection of springs for each DOF of the suspension system was performed by Gan Chowdhury and Sarkar [7]. The selection is based on the relationship:

$$K = \omega^2 M \tag{4}$$

Where K is the system stiffness, ω is the desired angular frequency in radians/sec, and M is the mass of the portion of the system in motion for a particular DOF. The springs that were

selected in this current study allow the inertial mass to vary from 8 to 12 kg and the inertial mass moment of inertia to range between 3×10^{-2} and 12×10^{-2} kg m^2.

Other considerations regarding frequency pertain to the dependency of the flutter derivatives on the frequency of oscillation of the section model. As previously stated, the flutter analysis is performed by using experimentally obtained flutter derivatives in the frequency domain. Aeroelastic stiffness is revealed through changes in frequency. Aeroelastic stiffness results in the flutter derivatives H_3^*, H_4^*, A_3^*, and A_4^*. A model subjected to forced oscillation at frequencies other than the natural frequency could cause changes in the flutter derivatives from those of a model tested using a free-vibration system.

The mean angle of attack for the section model with respect to the free stream velocity has some effect on the static and dynamic responses of the model. Change in mean angle of attack changes the effective cross-sectional shape of a model facing the wind. This influences the coefficients of lift, drag, and moment for the model due to pressure distribution changes. Change in mean angle of attack results in higher peak angles for a given amplitude and a different interaction with the flow depending on the shape of the section model and the degree of the mean angle of attack. Complete separation of flow at high angle of attack could result in further instability and modified behavior of a model. Therefore, important attention must be given to setting the model at zero angle of attack (AOA) at zero wind.

Model Parameters

Great importance is placed on model design to allow for proper system operation. As stated earlier in the section on the effects of frequency, the mass of the system is critical for obtaining a frequency of oscillation for the expected reduced velocity range. The model

must also correctly represent the full-scale structure while maintaining enough stiffness at the scaled-down size needed to fit in the wind tunnel test section. The section model stiffness must be high to prevent any change in shape of the model as wind speed increases. The model length for the ISU WiST Lab Bill James Wind Tunnel can be at the most 21 in. long so as to allow accommodation of the section model in the suspension system. As with all wind tunnel model design, blockage is an important concern for prevention of any significant changes to the airflow in the test section. The effective cross-sectional area of all bridge deck section models tested in the Bill James Wind Tunnel have been kept at a range of five to eight percent of the test section cross sectional area.

2.4 Past Work

Review of System Identification Methods Employed

A variety of system identification (SID) methods have been applied concerning aeroelastic studies. A modified Ibrahim time domain (MITD) method was developed by Sarkar [8] to extract direct and cross-flutter derivatives from the coupled free-vibration data of a two-DOF section model. Sarkar et al. [9, 10] successfully identified eight flutter derivatives from noisy time-history-displacements generated during laminar and turbulent flow.

Many other (SID) methods were employed over the course of dynamic flow analysis history. These methods were the least squares (LS) method, instrumental variable (IV), maximum likelihood (ML), and extended Kalman filtering (EKF). Imai et al. [11] have reviewed the aforementioned methods. Hsia [12] elaborated on different (LS) algorithms for system parameter identification. Yamada and Ichikawa [13], Diana et al. [14], Iwamoto and

Fujino [15], and Jones et al. [16] have used (EKF) methods for solving structural dynamics problems. Jakobsen and Hjorth-Hansen [17] and Brownjohn and Jakobsen [18] used the covariance block Hankel matrix (CBHM) method to extract parameters of a two-DOF dynamic system. The CBHM method has also been extended to solve for three-DOF systems. The principles of the CBHM method have only been illustrated with the extraction of eight flutter derivatives in a two-DOF system [17, 18]. Other flutter derivative extraction performed by Gu et al. [19] and Zhu et al. [20] used a SID method based on unifying least squares (ULS) theory to extract flutter derivatives for a two-DOF model. The ULS method has the ability to extract all 18 flutter derivatives with the use of a three-DOF system.

Extraction of eight flutter derivatives from a two-DOF system has become commonplace in aeroelastic analysis. The flutter derivatives that can be extracted from a two-DOF system are H_1^*, H_2^*, H_3^*, H_4^*, A_1^*, A_2^*, A_3^*, and A_4^*. Flutter derivative extraction becomes increasingly difficult when the third DOF is added to the system.

ILS-System Identification Method Developed at Iowa State University

The iterative least squares (ILS) method developed at the Iowa State University WiST Lab has the capability of efficiently identifying all 18 flutter derivatives from a three-DOF free-vibration suspension system. The ILS method developed at ISU incorporates a digital filter for filtering noisy displacement time-histories and approximation of higher derivatives of displacement using finite difference formulation. The advantages of the ILS method are:

- A single computer program that is capable of solving flutter derivatives for a variety of combinations of single-DOF, two-DOF, and three-DOF cases.
- Stiffness and damping matrices are directly derived from acquired free-vibration displacement time-histories and numerically generated velocity and acceleration time-

histories using digital filtering and finite differencing (thus avoiding extraction of eigenvalues and eigenvectors).

- Accurate parameter identification can be performed when different combinations of degrees-of-freedom are used.

The flutter derivatives are extracted by an aeroelastically modified free-vibration equation of motion. Equation (5) is formed by substituting Equation (2) into Equation (1) and bringing all terms to the left hand side.

$$\underline{\ddot{y}} + \underline{C}^{eff}\,\underline{\dot{y}} + \underline{K}^{eff}\,\underline{y} = \underline{0} \tag{5}$$

Equation (5) can be represented in the state-space model as

$$\underline{\dot{X}} = \underline{A}\underline{X} \tag{6}$$

where

$$\underline{X} = \begin{Bmatrix} \underline{y} \\ \underline{\dot{y}} \end{Bmatrix}, \underline{A} = \begin{bmatrix} \underline{0} & \underline{I} \\ -\underline{K}^{eff} & -\underline{C}^{eff} \end{bmatrix}$$

The $\underline{A}$ matrix is a $2n$ x $2n$ square matrix, where n is the number of degrees of freedom, and $\underline{I}$ is the identity matrix of size n x n. If acceleration, velocity, and displacement data can be recorded for n degrees of freedom for at least $2n$ different instances of time, then the $\underline{A}$ matrix can be identified. The ILS system identification software, programmed in MATLAB, takes a measured noisy displacement time-history and numerically filters out high frequency noise using a 'Butterworth' filter. When the displacement data is digitally filtered, the numerically obtained velocity and acceleration time-histories will exhibit deviations from the expected velocity and acceleration time-histories. This effect is cancelled out by only using the middle-half of the numerically obtained time-history to extract the elements of the

$\underline{A}$ matrix. The $\underline{A}$ matrix from the zero wind case will produce the mechanical stiffness and mechanical damping matrices for the suspension system and section model. The effective stiffness and damping matrices can be obtained from the $\underline{A}$ matrix for non-zero wind cases. The frequency-dependent flutter derivatives can then be extracted from the flutter equations. Gan Chowdhury and Sarkar [3] used the algorithm on the following page to describe the flutter derivative extraction process for the ISU WiST Lab ILS system identification code.

The three-DOF elastic suspension system developed in the ISU WiST Lab Bill James Wind Tunnel was originally designed and constructed as part of a senior research project as well as a requirement for the doctoral dissertation of Arindam Gan Chowdhury. The basic configuration of the suspension system is shown in Figure (3). This system was incorporated into a test section with cross-sectional dimensions of 36 inches (width) and 30 inches (height). The suspension system allows movement in the vertical, torsional, and lateral directions. Since this system is of free-vibration type, the effect of coupling between each separate DOF can be viewed when the section model is immersed in a dynamic flow condition.

The free-vibration suspension system utilizes linear air bearings riding on precision polished steel shafts for the vertical and lateral motions. The pneumatic bushings help to minimize friction to lower mechanical damping. Two torsional assemblies, one for each side of the suspension system, make up the components required to allow the torsional-DOF. Each DOF is controlled by a set of springs; the vertical-DOF contains a total of 16 springs, four at each corner; the lateral-DOF uses four springs; and the torsional-DOF utilizes four springs, one on each end of two torque bars. The selection of spring stiffness and size was critical for proper tuning of the system.

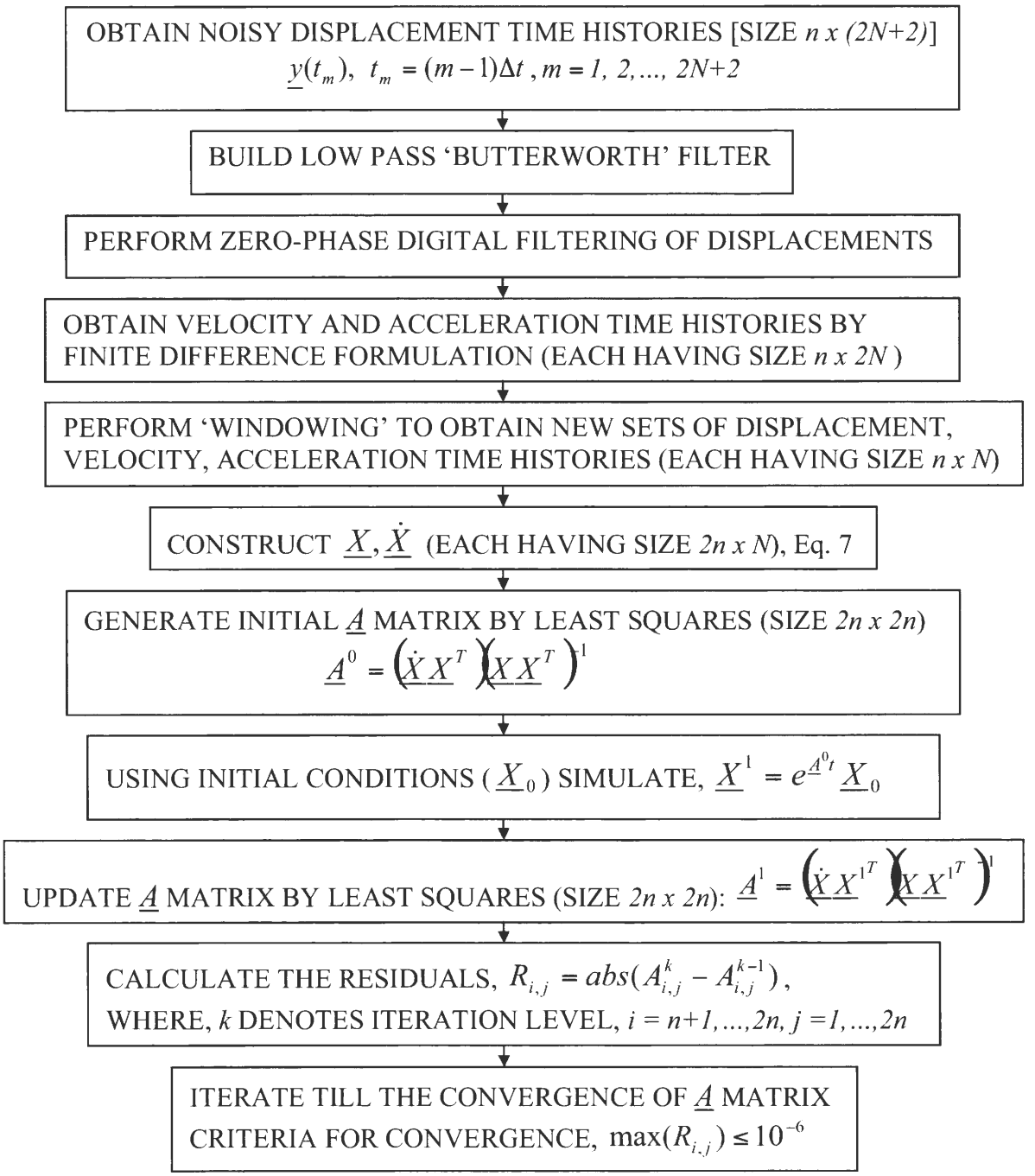

Figure 6. ILS system identification algorithm developed by Gan Chowdhury and Sarkar [3]

Of the torsional assemblies, one houses a torsional force transducer, while the other torsional assembly has a mock transducer. The vertical and lateral displacements are recorded with linear force transducers. A pair of linear transducers is used for both the lateral-DOF and the vertical-DOF. These transducers measure the amount of force in the spring in which they are attached. When the section model oscillates, this causes either a stretch or relaxation of the springs depending on the relative movement of the model with respect to the location of the spring. The data acquisition software has been designed to convert the measured forces into displacements based on the stiffness of the spring connected to the force transducer.

The linear force transducers each have a capacity of 11.34 kg (25 lb). The torsional transducer has a capacity of 1.152 kg m (100 lb-in). The torsional system consists of a shaft used to mount the section model, ball-bearings to support the model shaft, and two torque arms to transmit the torsional oscillation from the model to the torsional transducer. Torsional motion causes motion in the upper arm, the springs transfer this force into a linear force to the lower arm, and the force is then transformed back to a torque in the lower arm. Figure (7) illustrates the torsional assembly.

The initial condition system is contained on the underside of the suspension system test section. The initial conditions are set with the use of strings attached on one end to the section model end plates, and wrapped around a shaft with cranks on the other end. The displacement is made by turning the cranks to cause force in the strings, setting electromagnets to hold all strings, and simultaneously releasing all magnets. Figure (8) shows the initial condition apparatus. A separate crank for the initial condition system exists for each DOF.

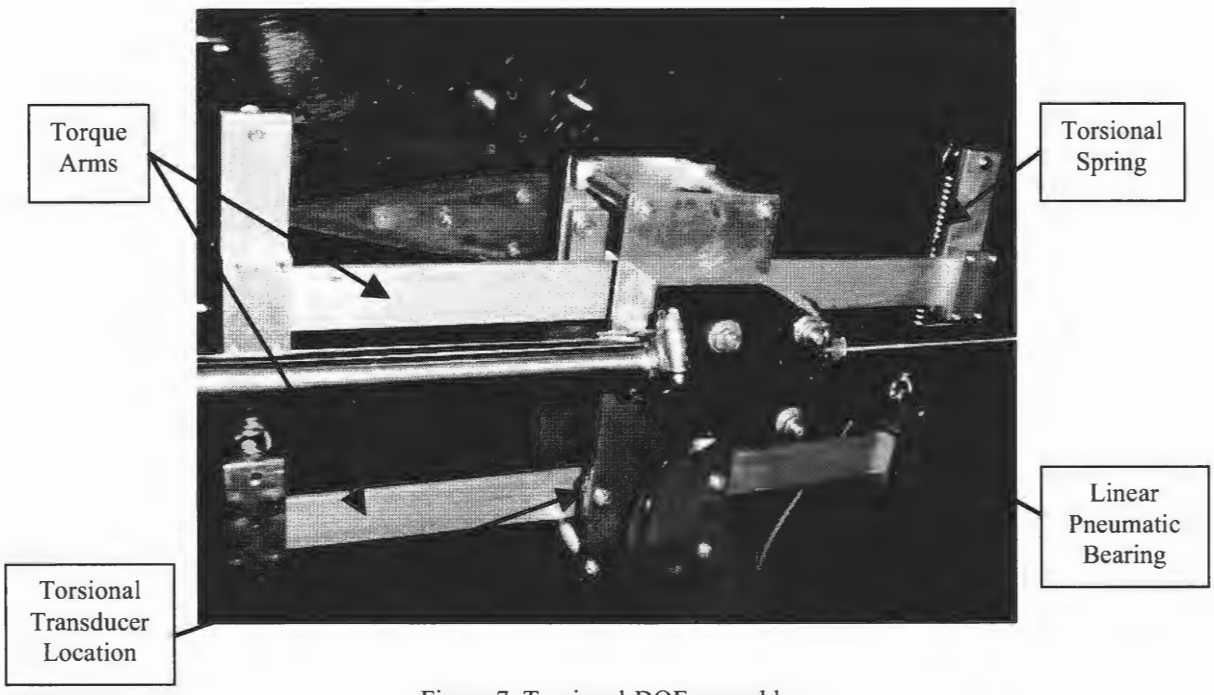

Figure 7. Torsional-DOF assembly

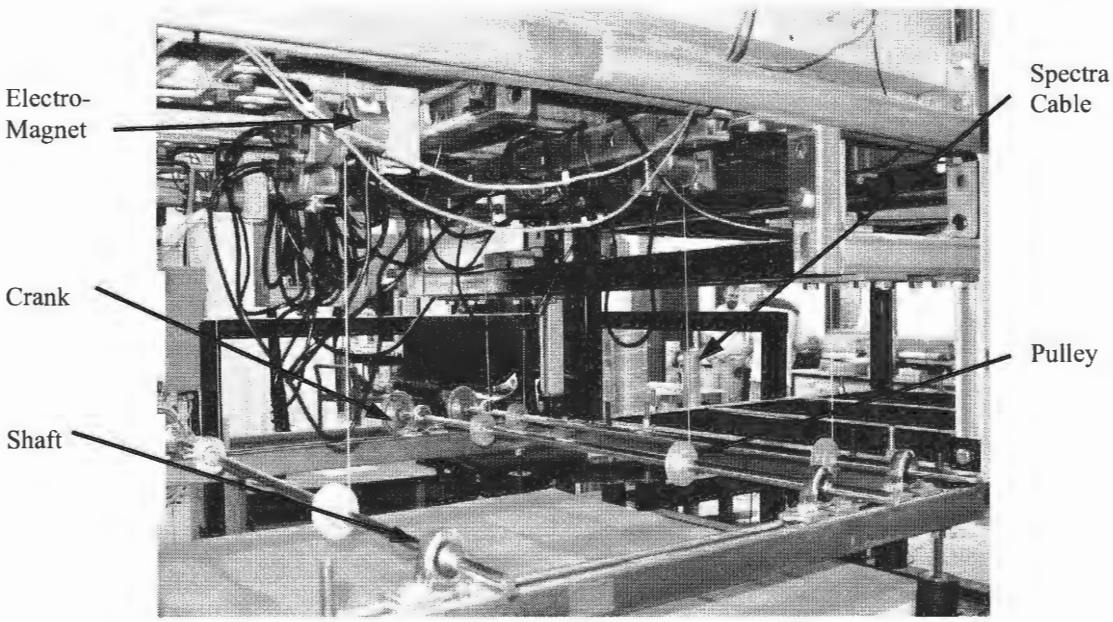

Figure 8. Free-vibration suspension system initial condition apparatus

The section models tested during the initial development of the three-DOF elastic suspension system for the ISU WiST Lab Bill James Wind Tunnel included a NACA 0020 airfoil and a streamlined bridge deck section model. The airfoil section model was used to validate operation of the suspension system, data acquisition system, and analysis method. The airfoil model had a chord length of 12 in. and a length of 21 in. The model is composed of a foam core with a fiberglass outer shell and plywood hardpoints for attaching the model to the suspension system. An illustration of the NACA 0020 airfoil section model is given in Figure (9).

The streamlined bridge deck model with semi-circular fairings has pressure taps incorporated into the design. The pressure taps allow an examination of the pressure distribution around the surface of the section model as it is subjected to aerodynamic loads. A study of the pressure distributions along the surface of the model as the model oscillates in a free-vibration system permits extraction of Rational Functions for the section model as well as flutter derivative extraction when used in conjunction with a forced-oscillation system. The streamlined bridge deck model was fabricated with acrylic panels for the flat surfaces, half-round acrylic pieces for the leading and trailing edges, and all-thread for stiffness and mounting of the model. Figure (10) is an illustration of the streamlined bridge deck section model.

The tests for the NACA 0020 airfoil and streamlined bridge deck resulted in an extraction of all 18 flutter derivatives. Both section models were tested for all three-degrees-of-freedom. Different combinations of single-DOF tests, two-DOF tests, and a three-DOF test were performed for comparison. The elastic suspension system in the Bill James Wind Tunnel allows movement in any combination of degrees-of-freedom simply by fixing

movement in the degrees-of-freedom where motion is unwanted. The possible DOF combinations and the flutter derivatives that can be extracted from these degrees-of-freedom are given in Table (1).

DOF Combinations	Extracted Flutter Derivatives
1-DOF, vertical	H_1*, H_4*
1-DOF, torsional	A_2*, A_3*
1-DOF, lateral	P_1*, P_4*
2-DOF, vertical and torsional	H_1*, H_2*, H_3*, H_4*, A_1*, A_2*, A_3*, A_4*
2-DOF, vertical and lateral	H_1*, H_4*, H_5*, H_6*, P_1*, P_4*, P_5*, P_6*
2-DOF, lateral and torsional	P_1*, P_2*, P_3*, P_4*, A_2*, A_3*, A_5*, A_6*
3-DOF	all 18 flutter derivatives

Table 1. List of flutter derivatives extracted from DOF combinations

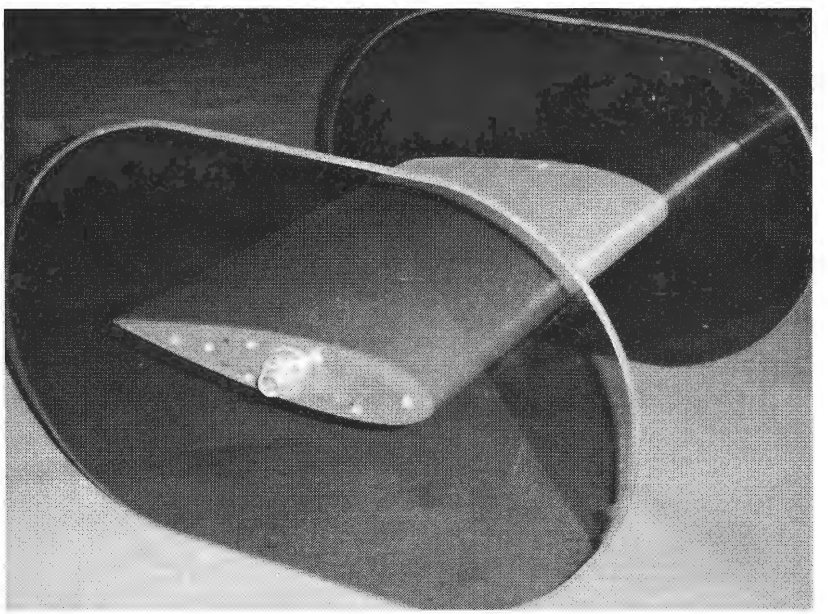

Figure 9. NACA 0020 airfoil section model used for suspension system validation

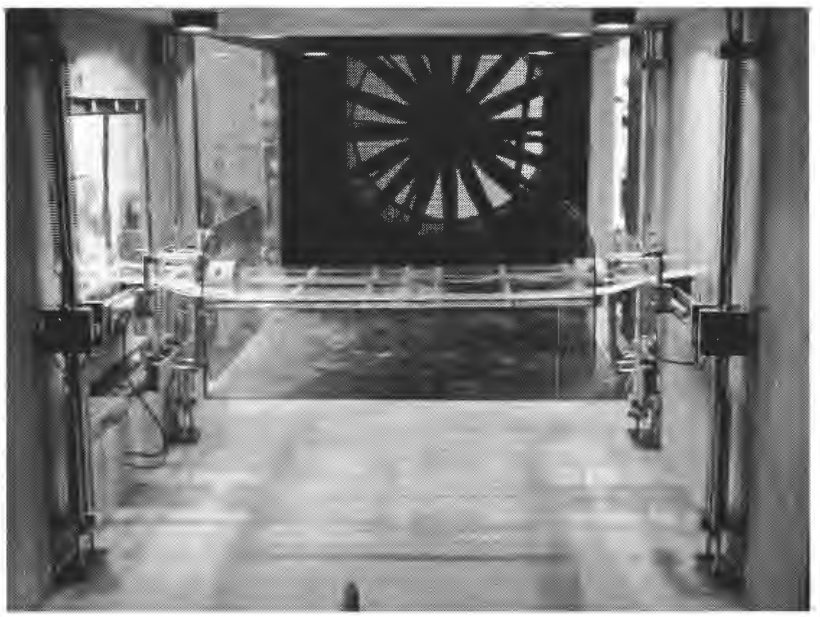

Figure 10. Streamlined bridge deck section model in suspension system test section

Prior to the tests involving validation of the three-DOF flutter derivative extraction from the elastic suspension system using the NACA 0020 airfoil section model, a numerical analysis was performed on the ILS system identification code. The analysis was accomplished by assuming stiffness matrices, damping matrices, and system mass for different DOF combinations. This analysis illustrated errors in the diagonal and non-diagonal stiffness and damping terms. According to Gan Chowdhury and Sarkar [21] the non-diagonal terms had higher percentages of error than the diagonal terms, and errors increase with an increasing number of degrees-of-freedom. For the experimental test, all 18 flutter derivatives were cross analyzed between single-DOF, two-DOF, and three-DOF to validate the operation of the flutter derivative extraction. A review of results from Gan Chowdhury and Sarkar [3] reveals consistency between the flutter derivatives from the different DOF cases for the NACA 0020 airfoil model.

Gan Chowdhury and Sarkar [3] claim that the 18 flutter derivatives for the streamlined bridge deck show similarities between the varieties of DOF cases. The vertical and torsional flutter derivatives show the greatest similarities. The vertical and torsional flutter derivatives were also compared with data from the Tsurumi Bridge deck two-DOF case, and showed similarity in this comparison. As stated earlier, the difficulty of flutter derivative extraction becomes increasingly difficult as more degrees-of-freedom are added to the analysis. The lateral flutter derivatives, P_1^* and P_4^*, showed some difference between the DOF cross-comparison.

Chapter 3: Experimental Procedure

3.1 Wind Tunnel Setup and Test Section Preparation

Extensive planning and preparation including the section model, the wind tunnel, and the free-vibration elastic suspension system precede any flutter derivative extraction tests. The ISU WiST Lab Bill James Wind Tunnel is an open-circuit wind tunnel with modular sections. The modular test sections allow preparations to be made inside a test section while it is not being used. This permits usage of the wind tunnel while the set-up of another experiment is ongoing.

The free-vibration / forced-oscillation test section is used for aeroelastic studies of section models. Figure (11) shows the Bill James Wind Tunnel with the free-vibration test section in place without the forced-oscillation apparatus. The data acquisition equipment is placed on a platform next to the wind tunnel. Figure (12) shows the interior of the free-vibration test section with a suspended model. Additional details of the elastic suspension system are provided by Sarkar, Gan Chowdhury, and Gardner [7].

A section model must be fitted with a model restraining mechanism prior to its placement inside the test section. The restraining mechanism helps to attach the section model rigidly to the elastic suspension system while allowing torsional and translational motions of the model and it also allows adjustment of the angle of attack of the section model. Figure (13) shows the restraining mechanism that bolts to the section model endplates. The endplates are fastened to the model before it is attached to the suspension system. Once the model is placed inside the test section, its angle of attack is adjusted and then the restraining mechanism is tightened. Once the test section is ready, it is moved into place in the wind tunnel.

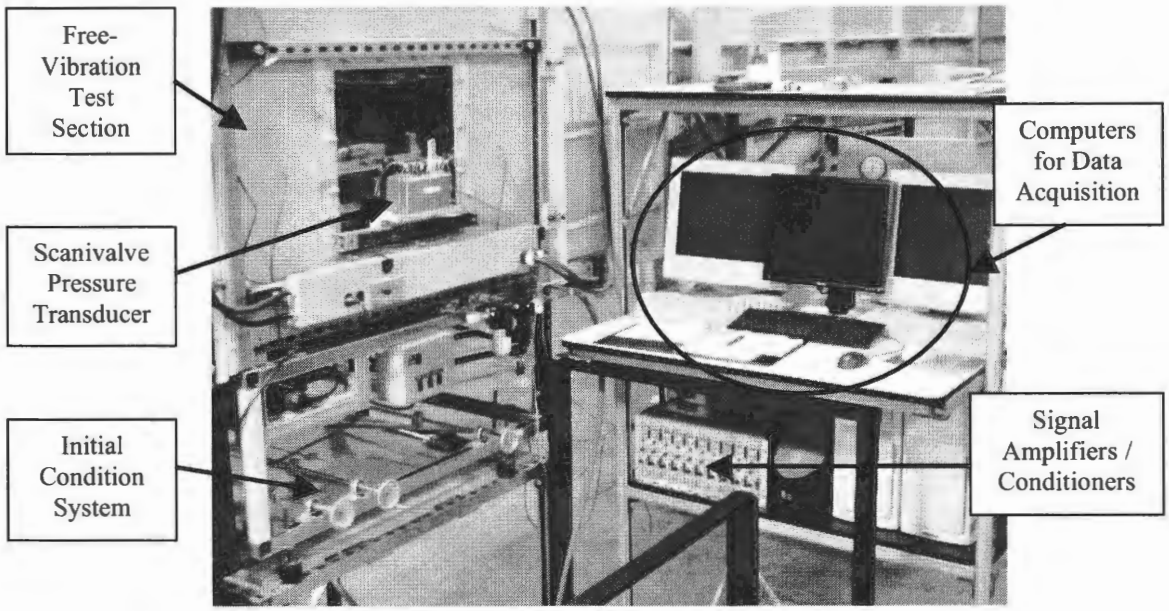

Figure 11. Free-vibration test section and data acquisition equipment

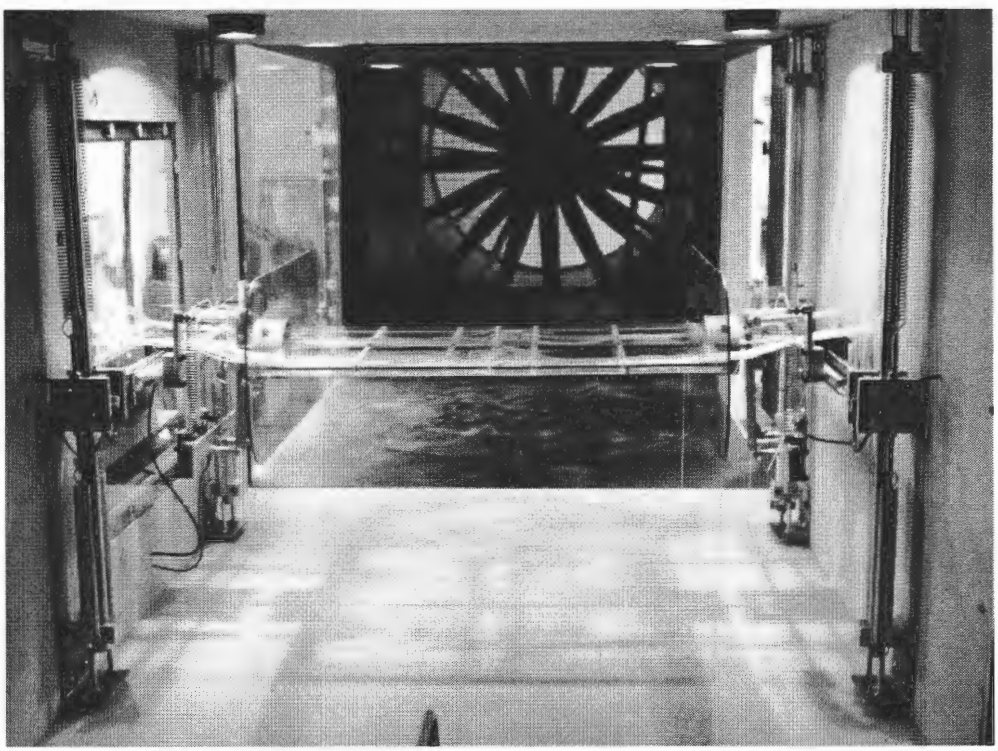

Figure 12. Free-vibration test section interior with suspended section model.

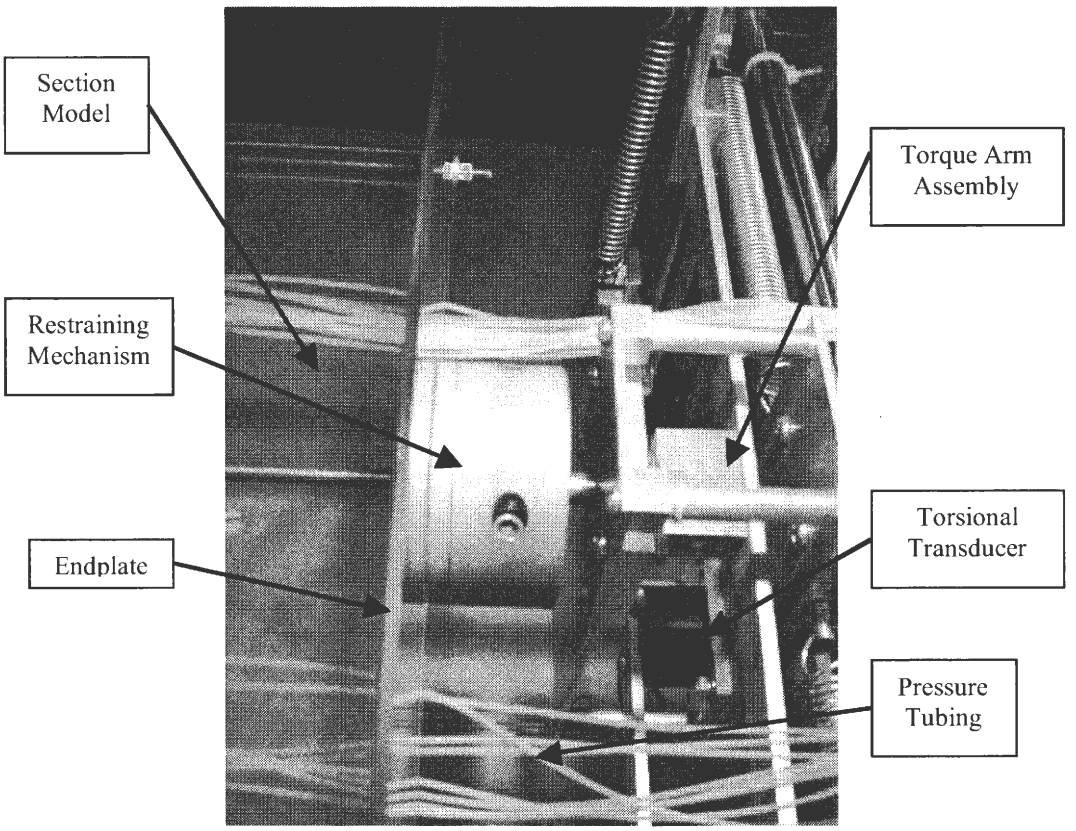

Figure 13. Section model restraining mechanism

After placing the test section in the wind tunnel, the data acquisition equipment and power supply cords for the test section must be connected. Depending on the type of test, single-DOF (vertical or torsional) or two-DOF (vertical and torsional), one or two degrees-of-freedom need to be restrained from motion. Translational motion is fixed by placing a piece of Tygon® tubing over the polished shafts on both sides of the pneumatic bearing that allows this motion. An adjustable clamp is then tightened over the tubing. The tubing helps to prevent scratching of the polished shafts from the clamps.

Fixing the torsional-DOF involves removal of the four springs that assist the torsional motion, and replacing these springs with a pair of washers fixed together by polyethylene string. This method is similar to the prior method for fixing the torsional-DOF. The

previous method involved wrapping string around each of the pairs of attachment points when a restriction of movement was required. The string only allows a certain separation distance between the two washers. The washers are placed over the bolts that would normally fix the ends of the torsional control springs. This modification, as well as many others, was performed to expedite the set-up for testing of multiple section models and multiple combinations of degrees-of-freedom.

The preparation for the initial condition mechanism involves attachment of four strings (for vertical and torsional initial conditions) between the model and pulley/crank system and adjusting these strings to the same tension. The tension adjustment is more critical between the two sides of the section model, since each cranking rod controls displacement of either the front side or the backside of the model. Refer to Figure (8) and Figure (14) for clarity. A physical measurement is taken at each of the four corners of the section model at zero-displacement, and then the model is displaced to a random amplitude,

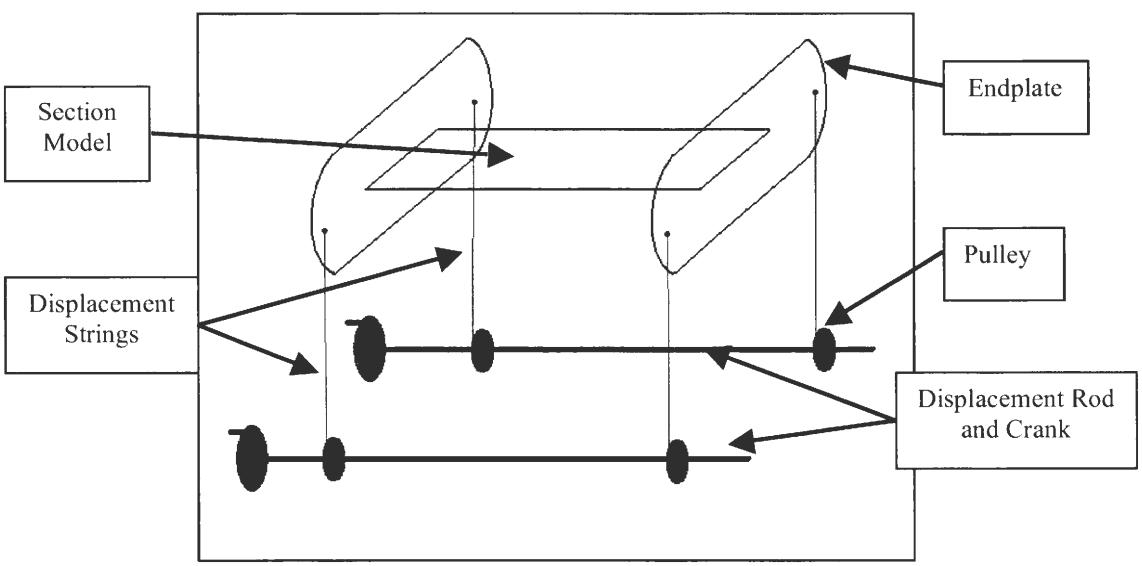

Figure 14. Initial displacement assembly

and the measurements of the corners are taken again. These measurements were taken with a measuring tape between a selected point of the ends of each endplate and the test section floor. The difference between the two measurements gives the total displacement for each of the four corners. After the displacement of each corner is known, the corners are adjusted so that displacements pertaining to each pair of strings on a rod and crank assembly are similar.

Initial displacement adjustments are important for correct operation of the free-vibration elastic suspension system. If the model is not displaced evenly from one side to the other, then the model will not oscillate freely. Other observations during testing of an improperly adjusted model included a rolling motion upon release of the electromagnets and binding of the pneumatic air bearings. The rolling motion is characterized by a rotational motion about the centerline of the model along the wind direction. This undesirable effect causes model damping characteristics to change from the expected.

3.2 Model Design and Fabrication

As stated in chapter 2, model design and fabrication methods need to cater to the type of testing as well as geometric complexity of the model. Since only displacement data is gathered in a free-vibration method, the addition of pressure taps in the model is not needed. If Rational Functions need to be extracted or the intention is to test the model in a forced-oscillation system, then pressure taps need to be incorporated in the model design. Usually, the procedure for addition of pressure taps is simple and involves making holes on the surface of the section model to attach flexible pressure tubes from the inside of the model to the holes directly or to rigid pressure tubes fixed inside these holes. In more complex geometries, the same procedure could be more involved. In this case, addition of pressure

taps would require design of the model using a CAD system in which the taps and tubing become an integral part of the model, and then producing the model with a rapid prototyping (RP) system. A variety of approaches for model design and fabrication were used during this research project.

The scope of the current research project was to improve the ILS method for flutter derivative extraction and test its robustness as well as to explore and use different model designs for the planned tests. Section models of four different bridge decks representing both bluff and streamlined shapes were used for the tests. These section models included cross-sections of (a) a bluff-body box girder bridge, (b) a streamlined box girder bridge, (c) a streamlined-split box girder bridge, and (d) a Π-shaped bridge section. A model of the Tacoma-Narrows Bridge was also designed to further develop model-building techniques for more complex geometries. The Tacoma-Narrows section model design and construction was intended to help understand methods for model production for future tests involving more complex model geometries.

Previous tests conducted for flutter derivative extraction in the ISU-WiST Lab, prior to the technique reported here, involved building models with conventional techniques by using common materials. This worked well since the models had simple geometries. The first tests administered for this research also involved models of simple geometry. These models included a rectangular box girder, a streamlined box girder, and a split-streamlined box girder bridge deck. These models were built from an assortment of materials such as wood, acrylic, and metal. Due to simple geometries of these models, pressure taps could be manually placed in any model when acquisition of surface pressures was needed.

The most important requirements for section model design involve its weight and stiffness. The rectangular box girder bridge was constructed with a combination of acrylic and metal where acrylic was used for the central part of the model. The acrylic eased the placement of pressure taps and also aided in keeping the model weight to a minimum. This section model had pressure taps so that pressure data could be acquired for Rational Function analysis and for future testing in forced-oscillation situations. This model was tested twice with two different lengths to study the effects of model length on flutter derivatives.

Two pieces of threaded rod were placed through the center of the rectangular box girder model to provide attachment points for placing the model in the elastic suspension system and to add to the rigidity of the model. Rigidity is an important issue when conducting dynamic testing. If a model flexes as it undergoes aeroelastic-induced motion, then the dynamic response characteristics would change drastically. Pressure taps were placed into the model by drilling holes along its centerline (in the along-wind direction) through the acrylic part of the model. Lengths of plastic tubing were inserted into the holes from inside the model surface and routed to the ends of the model. The tubes are connected to pressure transducers if pressure data acquisition was desired. Figure (15) shows the rectangular box girder section model in the initial configuration of 12 inches length. As part of a study to view the effects of model length on flutter derivatives, its length was increased to 21 inches. Figure (16) shows the longer model.

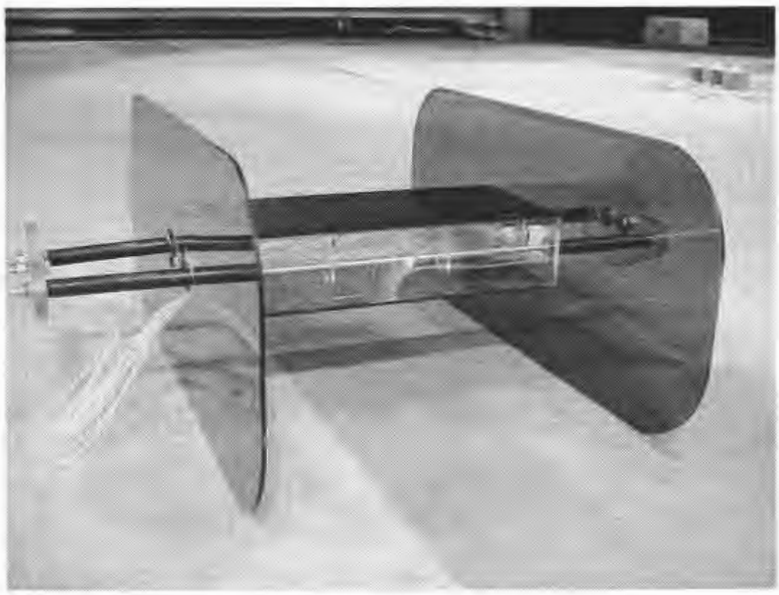

Figure 15. Twelve-inch rectangular box girder section model

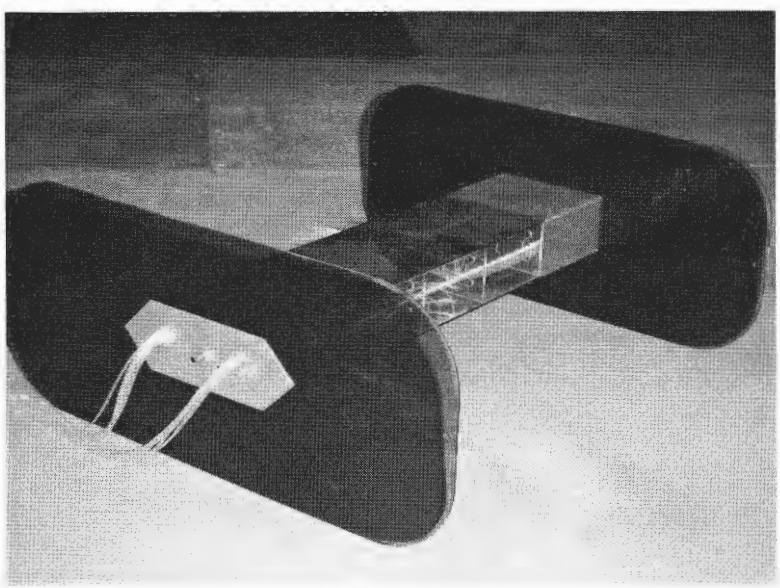

Figure 16. Twenty-one inch rectangular box girder section model

As stated earlier, weight is an important issue when designing models for dynamic testing. The elastic suspension system utilizes springs of a given stiffness. The stiffness of the springs combined with the mass of the oscillating system determines the natural

frequency of the system. This concept is illustrated by Equation (4) in chapter 2. The dependent variables in this equation are the system mass and the spring stiffness. In the case when the system mass is significantly changed, the system stiffness must be altered to maintain similar natural frequencies. Changing model weight to accommodate system frequency is an easier task by far than altering system stiffness. As seen by inspection of Figure (15) and Figure (16), when the length of the rectangular box girder model was changed, other changes were made to maintain nearly constant model weight. In the shorter model version, hollow steel tubes were used as spacers as well as added mass to control the natural frequency of the system. These tubes were removed in the longer version since spacers were not required and also to reduce overall mass to accommodate additional model mass.

When the requirements of the section models only constituted acquisition of displacement time histories, the models could be constructed using expedient and simplistic techniques. This also allowed model production with the use of conventional materials. Two section models of the four used in this research were made using this simpler style of construction. These models were the streamlined box girder bridge and the split-streamlined box girder bridge.

Both streamlined bridge deck models used for this research were composed of wood and metal. As with the rectangular box girder bridge deck, these models used threaded rod to provide rigidity to the models and, most importantly, a place to fasten the section models to the elastic suspension system. The bodies of the streamlined models were constructed as a lattice made out of wooden scrap for the skeleton and 1/8-inch plywood for the shell. Considerations were made to construct these models with acrylic and threaded rod, but it was

decided that pressure data would not be taken during the flutter derivative extraction tests. This construction technique kept the cost lower and allowed faster construction.

After assembly of the models, the surfaces of the models were filled and sanded to remove surface imperfections on the plywood. As with all section models produced for this research in the ISU WiST Lab Bill James Wind Tunnel, the end plate mounting points were placed in common locations to permit usage of one set of end plates with multiple models. Figure (17) shows the streamlined box girder bridge deck model. Figure (18) shows the split-streamlined box girder bridge deck model. Both models were constructed with a length of 21 inches.

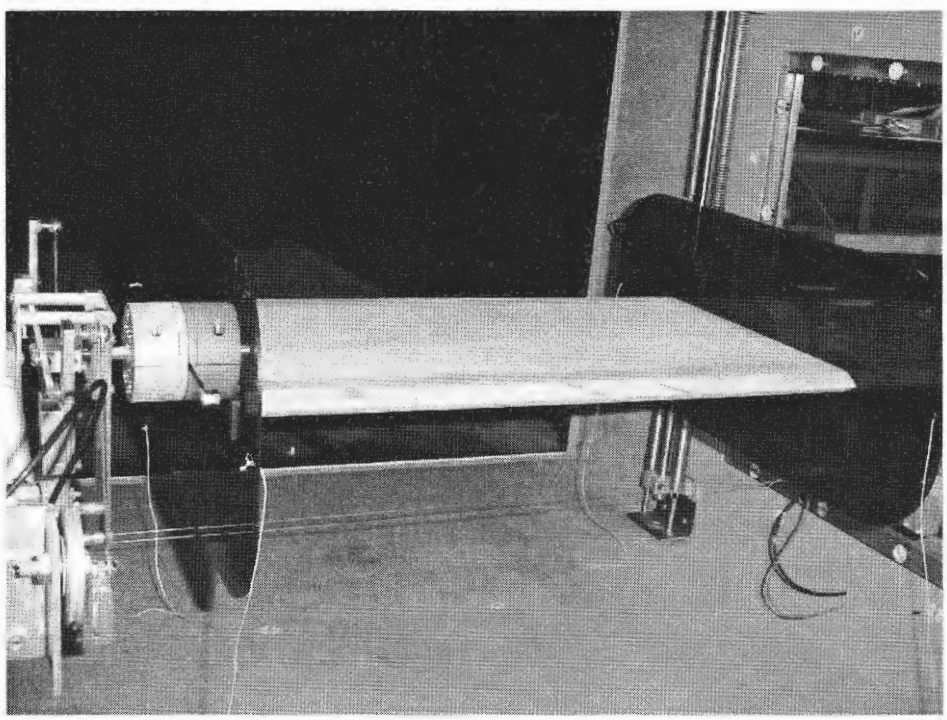

Figure 17. Solid-streamlined box girder bridge deck model

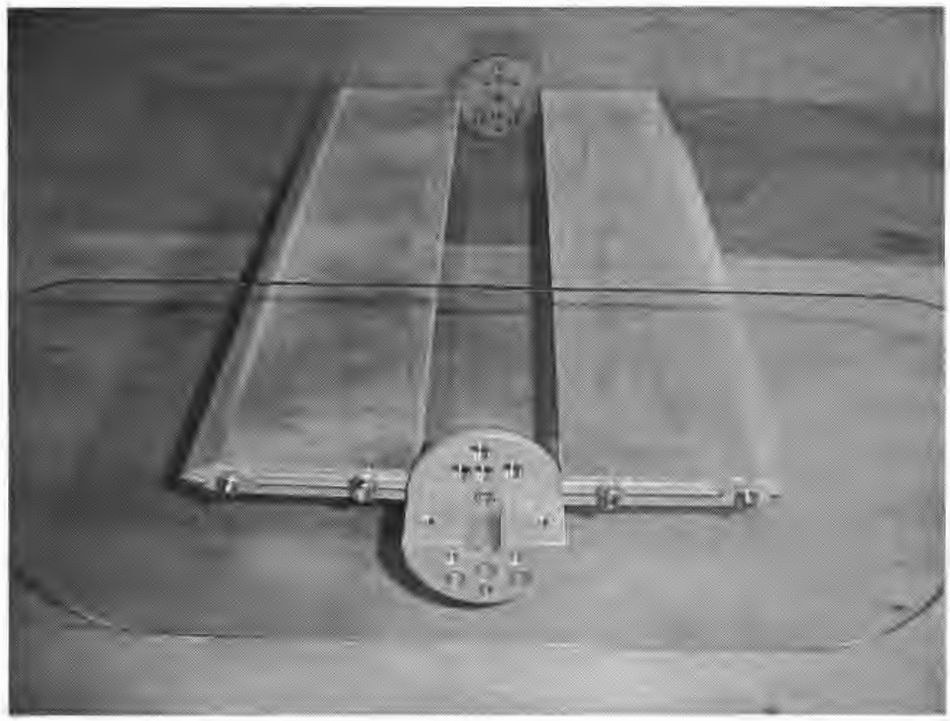

Figure 18. Slotted-streamlined box girder bridge deck model

More technologically advanced construction methods are needed on section models with complex geometries and those requiring pressure taps in areas where it is difficult to place such taps. The main goal of this research, with regards to section model production, involved entertaining the idea of using a CAD approach to produce models with a Rapid Prototyping or RP Machine. The Π-shaped Bridge was designed using this procedure, and then subjected to flutter testing. The initial design and construction phases for the section model of the Tacoma-Narrows Bridge were initiated using the CAD/RP approach to further standardize this method.

The CAD/RP approach to model production for the ISU WiST Lab uses SolidWorks to design the model and an RP machine to produce a 3D part composed of ABS plastic. Many considerations must be made during the design procedure to enable proper model

construction during the RP phase. Problems encountered during the RP process included material thicknesses and size limitations. The RP machine builds the part using a fine bead of near-liquid plastic continually fed in a pattern that results in the overall geometry of the section model. This bead has dimensions of 0.010 inches thick by 0.020 inches width, thus limiting material thicknesses to these sizes depending on build up orientation. Vertical thicknesses must be made on multiples of 0.010 inches, and horizontal thicknesses must be made on multiples of 0.020 inches. The vertical direction corresponds to the z-axis on the build platform, while horizontal direction corresponds to movement in the xy-plane on the build platform. The build platform dimensions are 10 inches wide by 10 inches long. This limits the overall dimensions of the part being produced in the RP machine.

The orientation of the model during the construction phase can be adjusted before starting the RP process. Orientation would be adjusted to allow for more efficient usage of the build platform dimensions, to limit the amount of support material the machine uses, to place support material in locations that allow for easy removal without damaging the part, and to correlate to the orientation used during the CAD process. The usable dimensions of the build platform are actually slightly smaller than the actual dimensions of the build platform. The CAD models were tailored to a build platform size of 9 ½" by 9 ½". Orienting models diagonally on the build platform allowed for longer model lengths.

Support material is a loosely constructed matrix of plastic placed in locations that would result in a cavity when the part construction is completed. In other words, if a section of the model doesn't contain material between itself and the build platform, support material is used to provide a surface for the RP production of the section. The support material must be removed after RP production is completed. Certain orientation of the model reduces the

amount of support material, therefore reducing the amount of raw materials used for the build. Strategic orientation of the model also allows for support material placement in locations that allow for easy removal without damage to the section model parts. Each of these considerations must be made during the initial CAD process to ensure the desired effect.

During the design and construction of the Π-shaped Bridge model, the main considerations pertained to the overall size of the section model. Most models used in the Bill James Wind Tunnel elastic suspension test section were designed with a length of 21 inches. This dimension exceeds the capabilities of the build platform. To accommodate the model on the build platform, the design would need to be sectioned. Reducing the model length to half would not help either because the depth and width of the Π-shaped Bridge deck exceeded the dimensions of the build platform. The model was produced with three sections to overcome this limitation. The surfaces between adjacent sections were staggered to allow for additional gluing area when joining the sections. Figure (19) shows the middle section of the Π-shaped section model. The complete CAD model is illustrated in Figure (20).

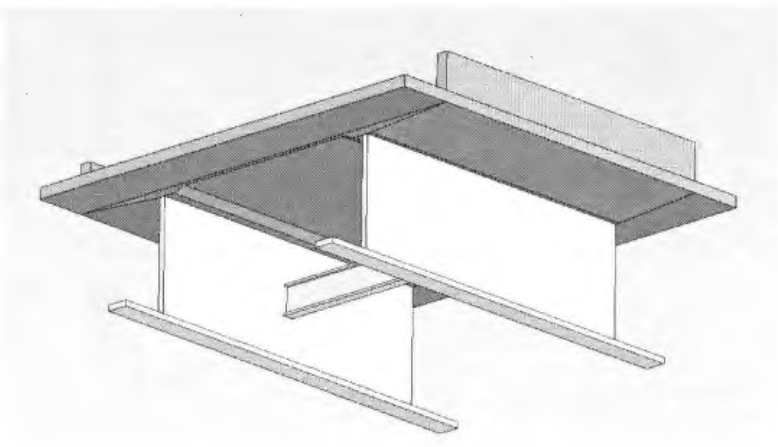

Figure 19. CAD middle section of Π-shaped Bridge deck model

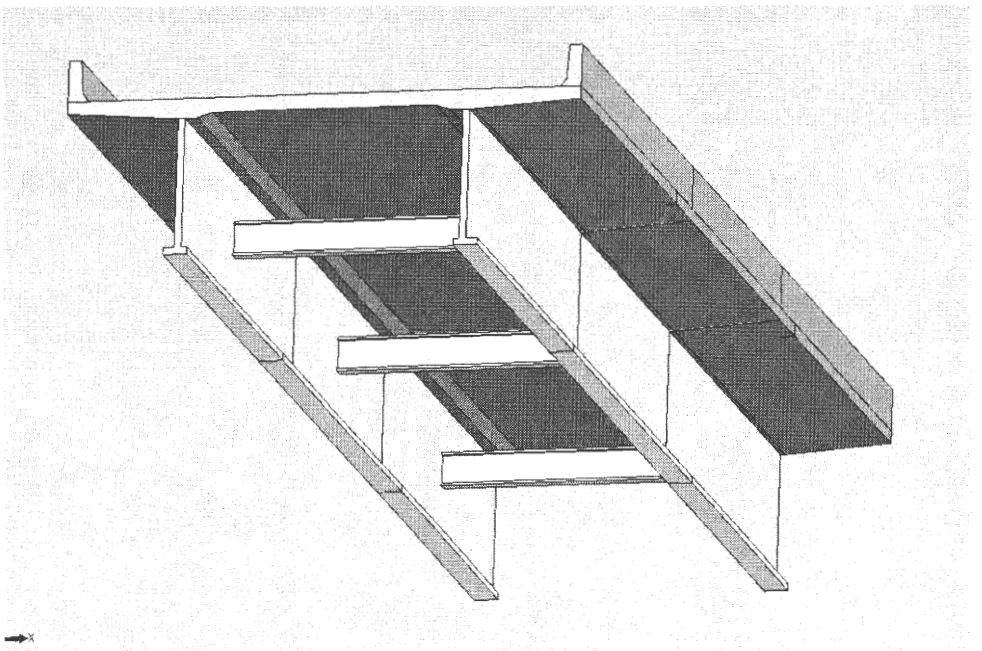

Figure 20. Complete CAD model of Π-shaped Bridge model

A minor problem experienced during the testing of the Π-shaped Bridge involved flexibility in the section model mount. As discussed previously, the system must be rigid to avoid movement other than what would occur for the DOF being studied. For the Π-shaped Bridge, four blind holes of about one inch deep were drilled at each end of the model in locations where material thickness permitted. Pieces of threaded rod 1-½ inches long were then epoxied into the holes for mounting the end plate and section model clamps. Large washers were used to secure the end plates to the section model. The washers did not suffice in suppressing the motion between the clamps and the model. The flexibility issue was resolved by adding aluminum plates to the outside surface of the end plates to increase the clamping force between the section model end and the end plate. The aluminum plates used to stiffen the connection between the section model and the elastic suspension system can be seen in Figure (21).

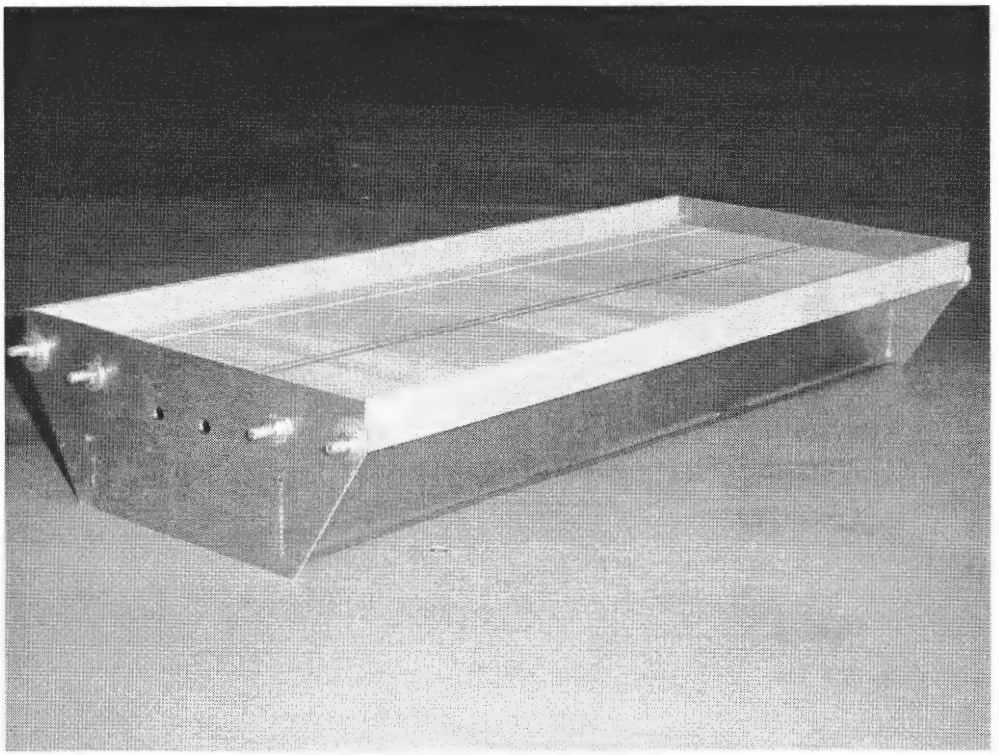

Figure 21. Π-shaped Bridge section model

The Π-shaped Bridge deck posed many issues not encountered during typical model construction, but the Tacoma Narrows Bridge Deck brought on many additional issues. The Tacoma Narrows Bridge model contains many I-beams that when scaled down have very diminutive thicknesses. In order to make the thicknesses of the I-beams more manageable for the RP machine, the thickness scale was made slightly larger than the model scale. Other problems with the construction of the Tacoma Narrows Bridge resulted from the difficulty of finding an orientation that would allow for minimum support material and placement of support material in locations in which it was easy to remove.

Initially, the Tacoma Narrows Bridge model was designed for rapid prototyping of the model in three sections in the same manner as the Π-shaped Bridge model. The issue of support material location had no ideal outcome. In every orientation of the model on the RP

build platform, there would exist support material hidden within the I-beams making up the support structure. This would pose a problem for removal of the support material without damaging the support beams. The final decision was to build the model as individual parts, separating out the individual I-beams and other parts needing rapid prototyping. These parts would then be glued together after the RP process. All large, constant cross-section parts, such as the road deck and sidewalks, would be constructed out of sheets of acrylic. This would keep model construction costs low due to expensive pricing of RP material. The CAD model of the complete Tacoma Narrows Bridge section model is depicted in Figure (22). The dimensions of each model and initial conditions used for each test are shown in Table (2).

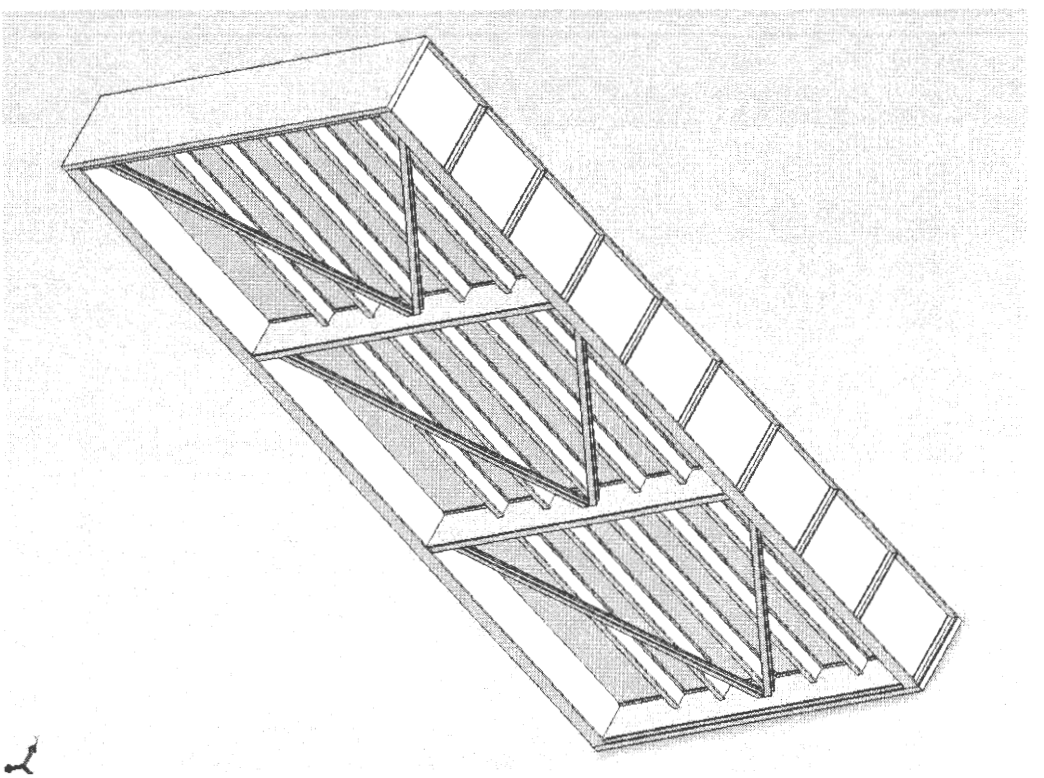

Figure 22. Tacoma Narrows Bridge complete CAD model

Bridge Deck Type	Dimensions (in)			Initial Displacement	
	Length	Width	Height	Torsional (degrees)	Vertical (in)
rectangular box girder (12 inch)	12	5	2.5	2.0 to 2.1	0.7 to 0.8
rectangular box girder (12 inch)	12	5	2.5	4.7 to 5.1	0.8 to 0.9
rectangular box girder (21 inch)	21	5	2.5	2.1 to 2.2	0.65 to 0.75
streamlined box girder	21	12	0.75	4.7 to 5.1	0.85 to 0.95
slotted-streamlined box girder	21	12	0.75	4.8 to 5.3	0.95 to 1.05
"Π" Bridge	21	7.5	3.25	2.0 to 2.5	0.6 to 0.7
Tacoma Narrows Bridge	21	11.4	2.25	N/A	N/A

Table 2. Dimensions and initial displacements of models tested and designed

3.3 Data Acquisition and Analysis

The flutter analysis software requires the input of displacement time histories to extract the stiffness and damping matrices of the dynamic system as well as the flutter derivatives. The displacement time histories were recorded using LabView data acquisition software. After processing these time histories to fix the starting amplitudes and time history length, the data was then read by the Iterative Least Squares System Identification (ILS System ID) software for the analysis. The ILS System ID software was initially developed and used by Arindam Gan Chowdhury as part of his Ph.D. dissertation under the guidance of Professor Partha P. Sarkar at Iowa State University. At the beginning of this research, the ILS System ID software was in its initial and basic software configuration. Most input variables that were used to analyze specific section models were hard wired into the code. This posed a problem when analyzing multiple bridge decks. With each new analysis, the

software user needed to update many variables while being careful in not overlooking any details.

The ILS System ID software improvement involved adding a title page, input prompts, and output graphs to the code. The title page becomes visible when a software user executes the program. Instructions for the time history input file format and titles are provided for the user at the end of the title page. The input prompts were designed to allow the user to input any variables that change from one analysis to the next. The input prompts involve variables such as the number of degrees of freedom, the time history length, amount of ensembles per velocity, number of velocities tested, the sampling rate of the data acquisition software, model mass per unit length, model moment of inertia per unit length, bridge deck span width, and system natural frequencies, etc. The output data configuration involves graphing of the flutter derivatives with respect to reduced velocity and providing the flutter derivative, stiffness, and damping matrices in a familiar form.

Some changes were also made to the formulation embedded in the ILS System ID software. Initially, all flutter derivatives for the multiple-DOF codes were calculated using the frequencies associated with the DOF with the lowest natural frequency. When comparing data with the flutter derivatives of similar bridge decks derived by Matsumoto [22] and Sato [23], flutter derivative values similar to the referenced sources resulted in most cases when using the frequencies for the DOF associated with the flutter derivative tied to that certain DOF. For the two-DOF (vertical and torsional) analysis, the vertical frequency was used for flutter derivatives H_1^*, H_4^*, A_1^*, and A_4^*. Thus, these flutter derivatives are plotted versus the reduced velocities calculated with vertical frequency at zero wind velocity. The flutter derivatives H_2^*, H_3^*, A_2^*, and A_3^* employ the torsional frequency. These are plotted versus

the reduced velocities calculated with torsional frequency at zero wind velocity. These changes as well as the previously stated changes helped improve analysis efficiency.

As part of the procedure of free-vibration flutter derivative extraction using the elastic suspension system and the ILS System ID software, the flutter derivatives are validated. The validation involves cross checking direct flutter derivatives between the single-DOF cases and the two-DOF cases and comparing the ISU WiST Lab Bill James Wind Tunnel results with flutter derivatives from Matsumoto and Sato. Favorable comparison will give confidence with the methods employed in the ISU WiST Lab. This current work helped to accomplish that confidence and at the same time raised more issues about the flutter derivatives and the techniques used to extract these derivatives.

The comparison of direct flutter derivatives involves obtaining flutter derivatives from single-DOF tests. The data acquired for this research included a single-DOF case in the vertical direction, a single-DOF case in the torsional direction, and a two-DOF case using both vertical and torsional motions. The flutter derivatives obtained with other extraction methods found in the literature were compared with those from this research, particularly data from models that were similar or exactly the same as the models used in the Bill James Wind Tunnel. The data from the multitude of sources was either given a visual qualitative comparison or plotted on the same graph to provide quantitative comparison.

Chapter 4: Results and Discussion

Considerable investigative efforts were placed on effects of section model parameters on model performance and flutter derivatives. This curiosity increased as research progressed. This chapter discusses the effects of section model length and initial amplitude on model performance and on flutter derivatives and it also gives a comparison of flutter derivatives between different types of bridge deck models. This includes a study of bridge decks that are bluff-shaped versus streamlined, streamlined box girder versus slotted-streamlined box girder, and aerodynamically unstable versus aerodynamically stable. Much of this work was conducted in hopes of standardizing the testing methods and the model building procedures for the ISU WiST Lab.

Except for the tests involving the study of different initial amplitudes, the amplitudes at initial conditions were comparable between all tests. For the vertical-DOF the initial amplitudes were between 16 to 18 mm. The vertical initial amplitude was 5.5% of the width of the streamlined models, 8% of the Π-Bridge width, and 13.3% of the rectangular box girder width. The torsional-DOF initial amplitudes were between 2 to 2.5 degrees. For the test involving the study of effects of initial amplitude, the torsional amplitudes were two degrees and five degrees. The initial amplitude study only involved a change in the torsional-DOF initial amplitudes. Table (2) in Chapter 3 shows the initial conditions.

4.1 Effect of Section Model Length on Flutter Derivatives

This part of the chapter discusses the effect of section model length on its performance. This study involved building a particular section model with a given length,

testing this configuration, changing the length of the model, and then testing the new model for comparison. The output data from the two models were compared to make note of similarities and differences between the two data sets. The data for both configurations were compared to data obtained from outside sources as well.

Two rectangular box girder section models with 12 in. and 21 in. lengths were used for this study. Figure (15) in Chapter 3 shows the model with 12-inch length. The model with 21-inch length is shown in Figure (16) in Chapter 3. The tests performed with each model included single-DOF torsional, single-DOF vertical, and two-DOF (vertical and torsional). As with each section model test, the single-DOF flutter derivatives of a particular section model were compared to the two-DOF flutter derivatives of the same section model to instill confidence in the operation of the system. The following charts in Figure (23) were used to compare the values of the direct flutter derivatives of the 12-inch and 21-inch rectangular box girder section models.

Upon inspection of the plots on the following page, it can be seen that the overall difference between the direct flutter derivative trends for the 12-inch and 21-inch bluff-body section models are minute. The tests reveal that the values of the flutter derivatives from each bluff-body configuration have increasing and decreasing values as well as peaks occurring in relatively the same reduced velocity value ranges. A larger difference between the 12-inch and 21-inch models exists for the torsional-DOF flutter derivatives.

End plates can have significant effects on model performance. The endplates create a three dimensional effect in the flow over the model. The sections of the model nearest to the endplates experience changes in the vertical and along-wind direction as well as horizontally (cross wind direction). The shorter a model in length, the greater the effect endplates have

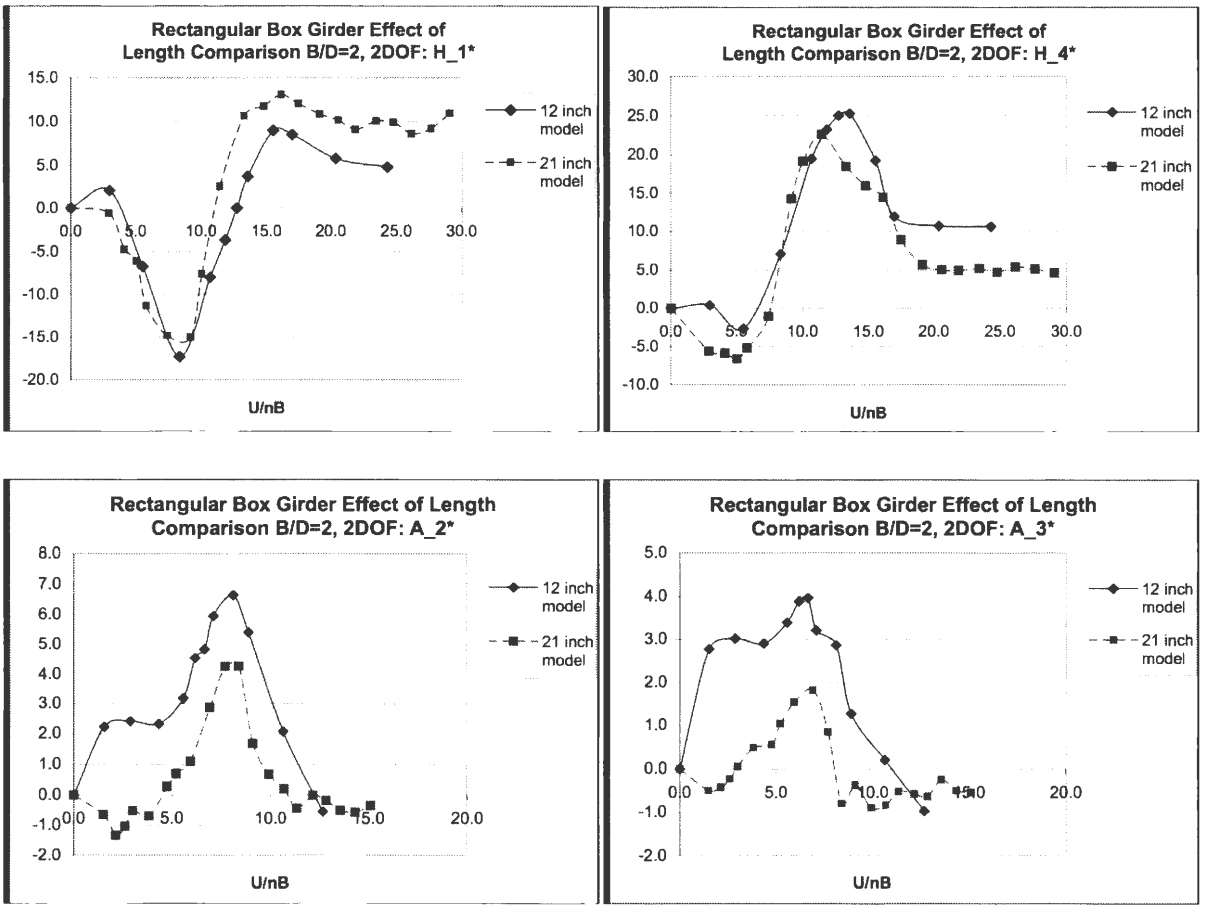

Figure 23. Direct flutter derivative comparison between 12 and 21-inch rectangular box girder models

on its behavior. More two-dimensional flow can be seen as the model length is increased. There exists a critical length at which further increases in model length do not provide significant reductions in the endplate effect. When this critical point is reached, further lengthening provides results similar to the critical length.

Aside from endplate effects, the torsional-DOF could also have been more affected by vortex shedding at the trailing end of the model. Vortex shedding becomes increasingly profound as a model becomes more bluff. Since the 21-inch model has a larger effective surface area between end plates and the two models have essentially equivalent masses, the airflow around these models would have a greater influence on the 21-inch model. The

lower amount of surface area on the 12-inch model would require higher velocity airflow to cause the same loading cases as the 21-inch model, but higher velocity airflows would also result in a change in the behavior of the vortex shedding. Changes in the vortex shedding could further affect how the model oscillates or could even prevent regular oscillatory motion from occurring. This would cause changes in the flutter derivative values due to variations in the aerodynamic damping characteristics. From this study, one could conclude that model length should be greater than a critical value to reduce the effect of the end plates.

4.2 Effect of Section Model Amplitude on Flutter Derivatives

The initial amplitude of oscillation was identified as an important parameter during testing and analysis of all of the section models involved in this study. The initial tests in this study were performed using similar amplitudes to those of tests performed in the Bill James Wind Tunnel before this study. Upon comparison of data from Matsumoto and Sato, it was realized that initial amplitudes used in this study were larger than those used by other researchers. This initiated an examination of data sets with different initial amplitudes.

The tests involving the effect of starting amplitude on flutter derivative values was performed on the rectangular box girder section model. This particular model was chosen for the section model test and configuration comparisons due to its inherent instability. Choosing proper guidelines for this particular model was most critical. Most problems associated with model design and model-testing parameters are magnified during bluff-body section model testing as opposed to testing streamlined models.

Since damping is amplitude dependent, damping characteristics of a section model will change when the starting amplitude is altered. Upon inspection of any particular

displacement time history from the free-vibration flutter analysis tests, one can observe the change in damping ratio as amplitude changes. This phenomenon is illustrated in Figure (24), which is of a sample displacement time history from the free-vibration system. The larger displacement time history is from the vertical-DOF, while the smaller displacement time history originated from the torsional-DOF. From examination of Figure (24), one can notice the change in damping as the amplitude decreases. This characteristic promotes the usage of similar starting amplitudes for consecutive tests to prevent inaccurate analysis.

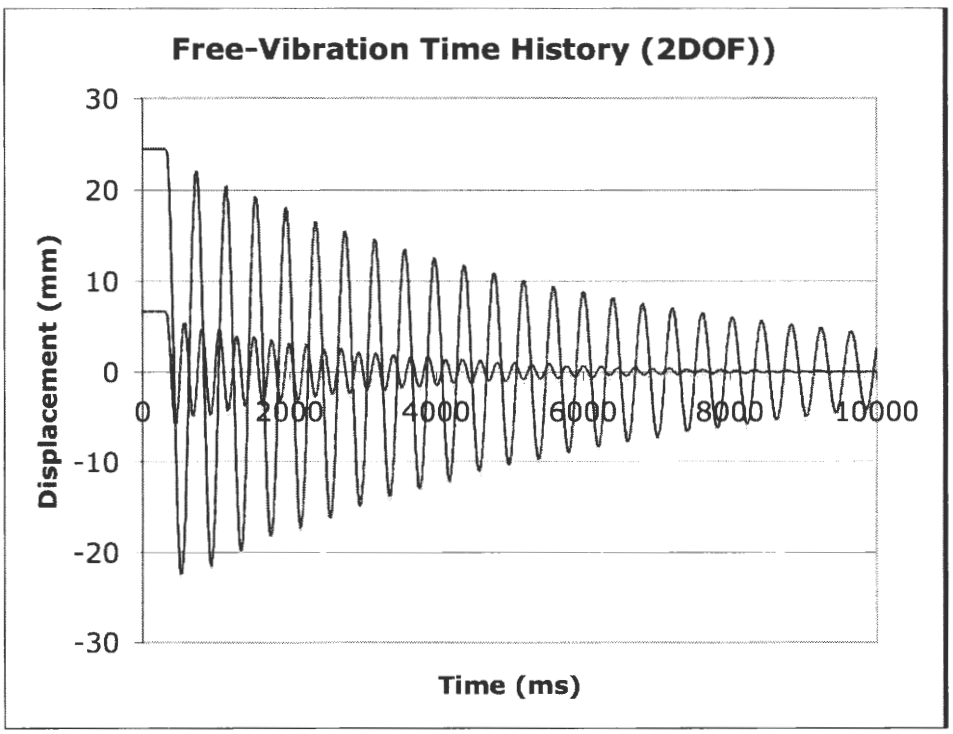

Figure 24. Typical free-vibration displacement time history

Figure (25a) shows the vertical direct flutter derivative output from the 2-DOF tests of the rectangular box girder section model. During this test, the initial torsional-DOF angular amplitude was changed from two degrees to five degrees. The vertical flutter

derivatives did not experience much change by altering the torsional-DOF initial amplitude. Small differences are noticed at reduced velocities higher than 13. These differences could exist at higher velocities due to larger lift forces associated with the velocities. A change in amplitude at the higher velocities would, therefore, impart more energy to the section model than at lower velocities.

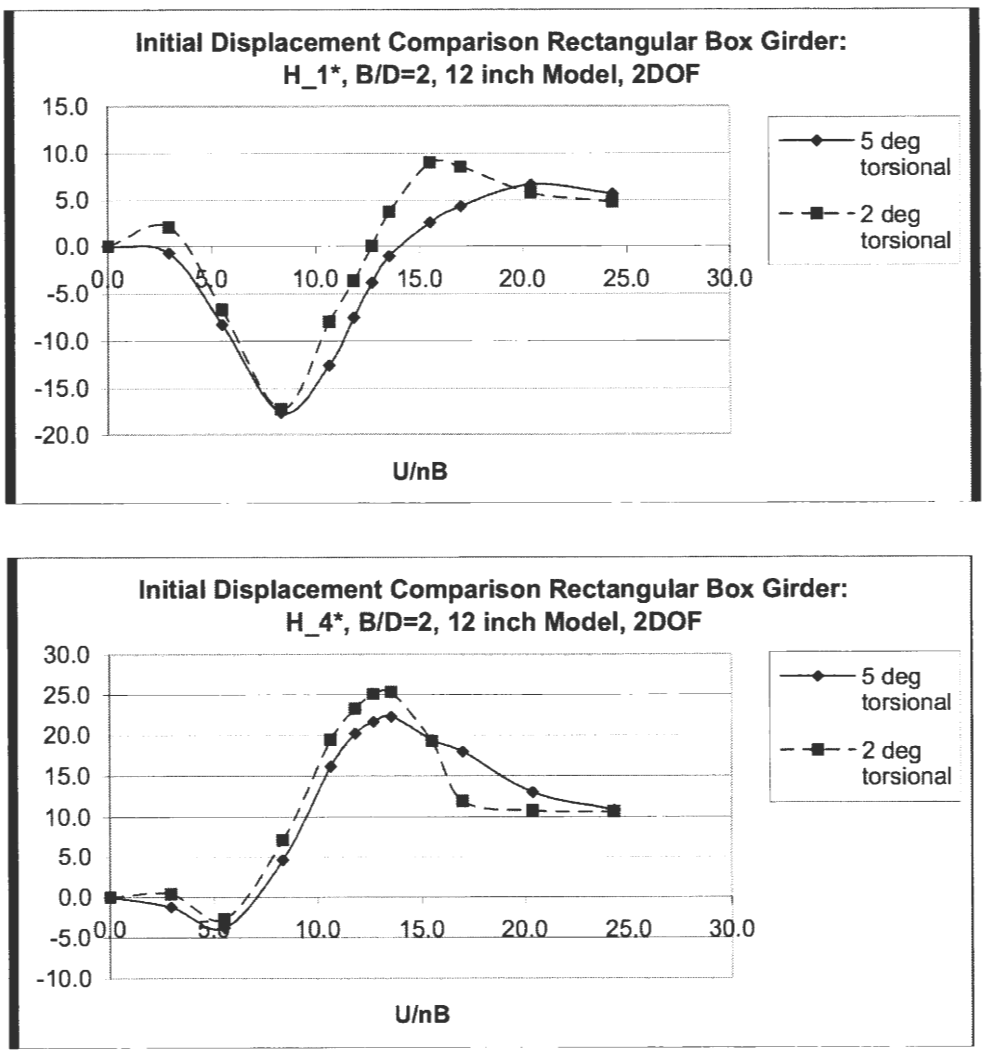

Figure 25a. Vertical direct flutter derivatives from rectangular box girder amplitude effect tests

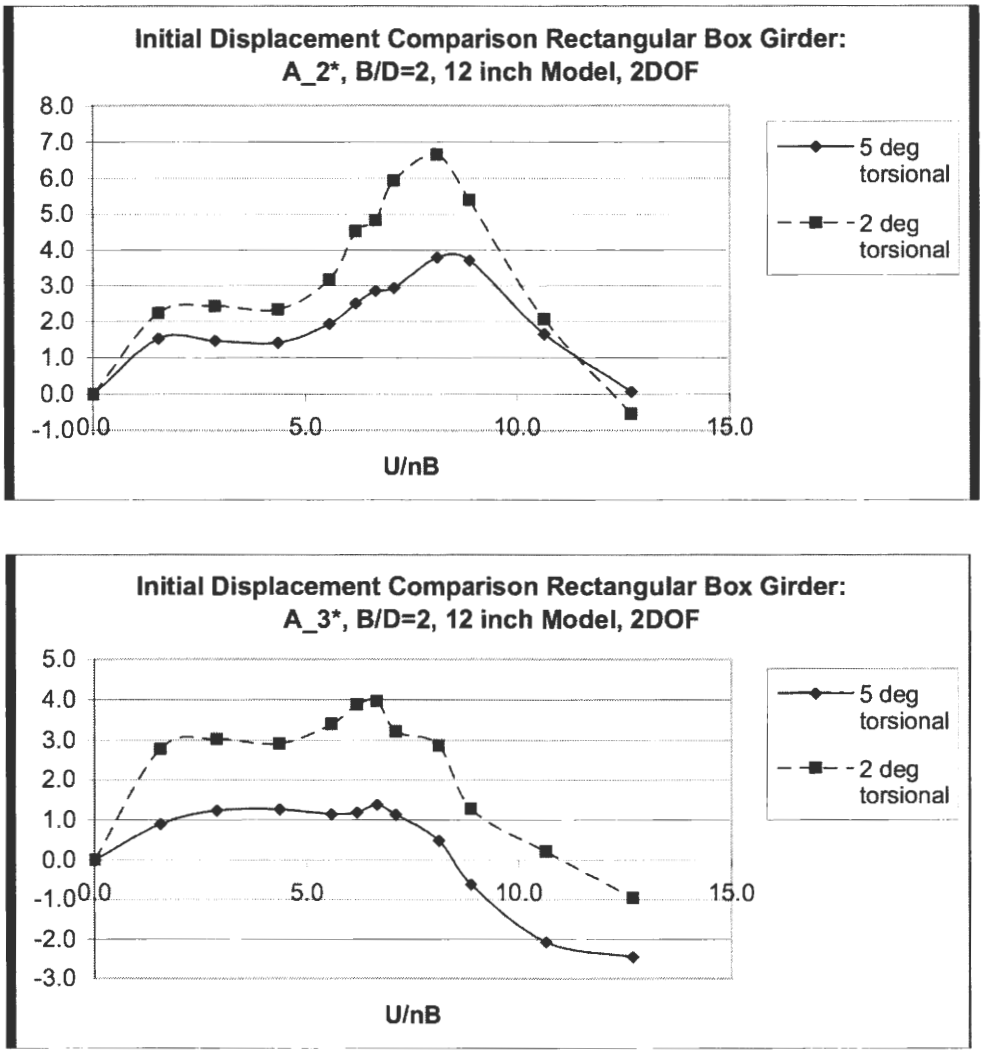

Figure 25b. Torsional direct flutter derivatives from rectangular box girder amplitude effect tests

Unlike the direct flutter derivatives associated with vertical-DOF, the ones associated with torsional-DOF were more greatly affected from the change in torsional initial amplitude. This can be noticed upon assessment of Figure (25a) and Figure (25b). From further inspection of Figure (25b), the initial amplitude can cause a change in flutter derivative values by 100 to 300%. Therefore, the choice of initial amplitude and keeping it constant for different reduced velocities during a series of tests are important considerations for ensuring sound and consistent results.

4.3 Comparison Study on Bridge Deck Types

Much of this research work was concentrated on developing and testing different types of bridge deck models, and using the results to perform comparisons on different categories of bridges. In the introduction it was stated that the main goal for studies on bridge deck flutter is to develop bridge deck cross sections that are inherently stable and therefore safe.

Once proper testing configurations and parameters were established, the elastic suspension system could be used to obtain data from a variety of bridge deck styles. The more user-friendly version of the ILS System ID software, as developed in this study, enabled easy acquisition and analysis of the newly acquired flutter data. This allowed extensive comparative studies of a variety of bridge deck configurations. The studies included comparison of bluff- versus streamlined- shapes of bridge decks, streamlined box girder versus slotted-streamlined box girder bridge decks, and stable bridge deck versus unstable bridge deck.

Bluff-Shape versus Streamlined-Shape

The first of the comparative studies involved an evaluation of the bluff-shaped (rectangular, B/D = 2) box girder model against the streamlined box girder model. Theory states that the streamlined box girder will exhibit stable characteristics, while the bluff-shaped box girder will be inherently unstable. The instability in the bluff-shaped box girder results from flow separation over the surface of the bridge deck model. This unattached flow causes extreme pressure inequalities between the upper and lower surfaces of the model at random intervals. The unattached flow also forms trailing-edge vortices. These vortices also disturb the natural oscillation of the model. On the other hand, a streamlined model

promotes little flow separation thus resulting in a more stable model. Figure (26a) shows the vertical direct flutter derivatives resulting from each type of bridge deck model. Figure (26b) compares the torsional direct flutter derivatives.

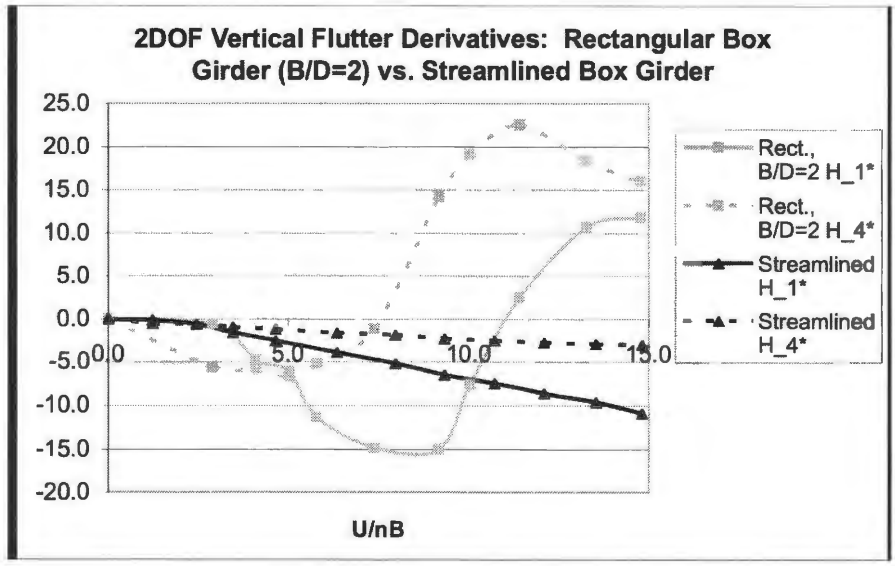

Figure 26a. Comparison of direct vertical flutter derivatives between bluff-shaped box girder and streamlined box girder

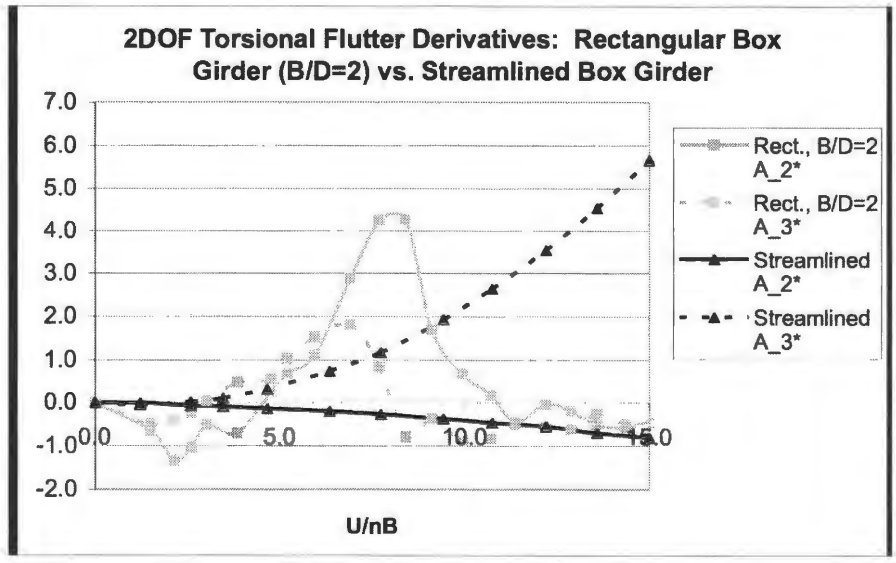

Figure 26b. Comparison of direct torsional flutter derivatives between bluff-shaped box girder and streamlined box girder

The vertical direct flutter derivative plot shows that the bluff-body bridge model is increasingly unstable as velocity is increased above a reduced velocity value of ten. Over the complete interval of reduced velocities the streamlined bridge deck model exhibits greater stability as the velocity increases. This would make the streamlined box girder design the ideal choice for stability in the vertical-DOF or galloping direction. In the torsional-DOF, the bluff-body model experienced great instability over the middle range of reduced velocities. The torsional direct flutter derivative associated with aerodynamic damping, A_2^*, for the streamlined bridge deck is negative and increases in magnitude as reduced velocity increases, adding more stability at higher wind speeds. A_3^*, the torsional direct flutter derivative associated with angular displacement or aerodynamic stiffness, increased in value as reduced velocity increased thus displaying a reduction in stiffness. This also shows that streamlined shapes do not experience "damping-driven" flutter but they are prone to "stiffness-driven" flutter.

The decrease in damping for the bluff-shaped section over the middle range of reduced velocities could result from trailing edge vortex shedding at a frequency close to the torsional natural frequency of the model. At reduced velocities out of the middle range, the vortex shedding could be occurring at a frequency that interferes with the natural oscillation of the model. These characteristics could be further investigated by performing flow visualization for the entire velocity range. With regards to stability, the streamlined box girder would be the best choice.

Streamlined Box Girder versus Slotted-Streamlined Box Girder

The bridge deck models associated with this portion of the research involved two section models both having streamlined characteristics. The difference between these

particular section models is that the slotted-streamlined box girder model contains a gap running lengthwise through the center of the model. The slotted box girder is shown in Figure (18) of Chapter 3, while the streamlined box girder is illustrated in Figure (17) of Chapter 3. The intention for testing two very similar models was to see the effects of opening up the center portion of the bridge to equalize the pressures over the top and bottom surfaces. Many modern bridge decks experiment with this principle as the slotted-streamlined box girder bridge design, but with different approaches. For instance, the Mackinac Bridge in northern Michigan uses metal grates as the road deck. This permits mixing of the airflow above and below the bridge deck.

In theory, a slotted box girder bridge should be more stable than a solid-streamlined bridge deck. The following charts in Figures (27a) and (27b) show the direct flutter derivatives resulting from the streamlined box girder and the slotted-streamlined box girder models. Each model test involved a single-DOF test for the torsional and vertical degrees-of-freedom, and a two-DOF test allowing movement in both the torsional and vertical degrees-of-freedom simultaneously. The following data is from the two-DOF test. From these output files, one could compare the stability of each bridge deck.

A qualitative analysis of the above graphs concludes the streamlined box girder performs slightly better for the vertical-DOF, while the slotted box girder is the superior performer in the torsional-DOF. All direct flutter derivatives, with the exception of A_3^*, exhibit increasing values in a positive sense as reduced velocity increases. The torsional direct flutter derivative, A_3^*, for the slotted-streamlined box girder shows a maximum value of about 50% of the maximum value for the same flutter derivative of the streamlined model.

These tests conclude that both models are almost equally stable with the slotted-streamlined box girder being slightly better than the streamlined box girder.

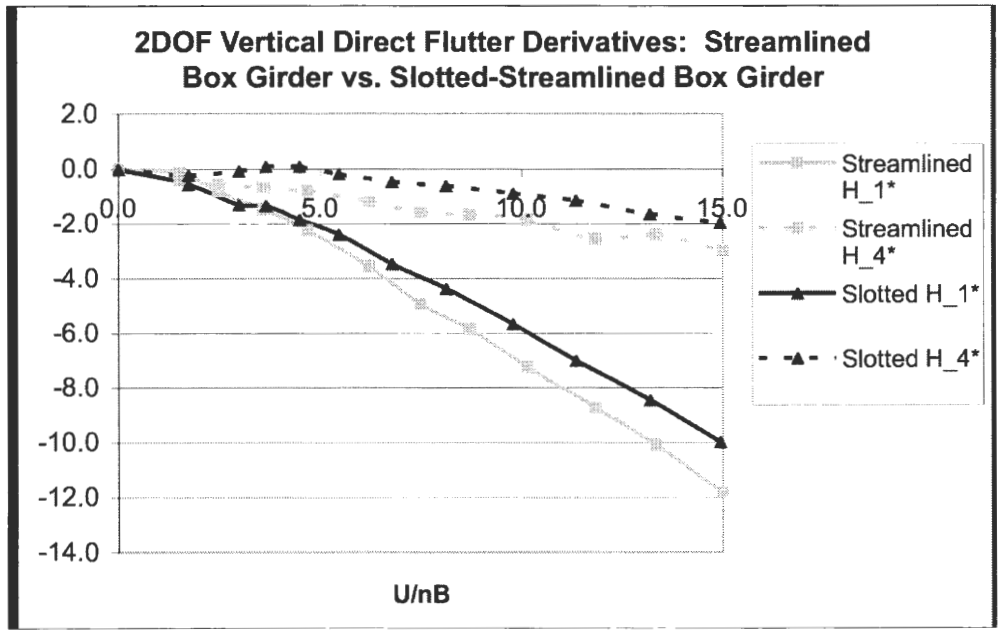

Figure 27a. Vertical direct flutter derivative comparison between streamlined and slotted box girder

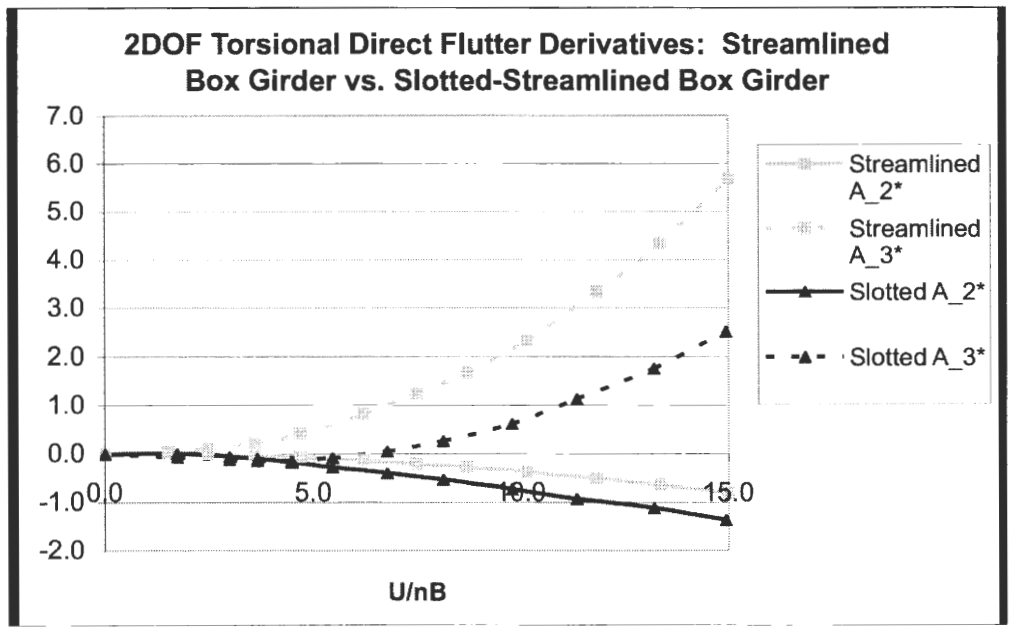

Figure 27b. Torsional direct flutter derivative comparison between streamlined and slotted box girder

Unstable Bridge Deck versus Stable Bridge Deck

The final bridge deck comparative study involves an overview of bridges tested during this research to increase understanding of stability in certain bridge deck designs. As previously stated, one of the main goals of bridge deck flutter analysis is to design safe and aerodynamically stable bridges. This work involved reviewing the data resulting from wind tunnel tests of all models used for this research, comparing the data sets, and rationalizing the behavior each model exhibited. The models included in this study were the streamlined box girder, slotted-streamlined box girder, rectangular (with B/D=2) box girder, and the Π-shaped bridge. The following plots in Figures (28a, b, c, and d) compare the direct flutter derivatives from each of the four models.

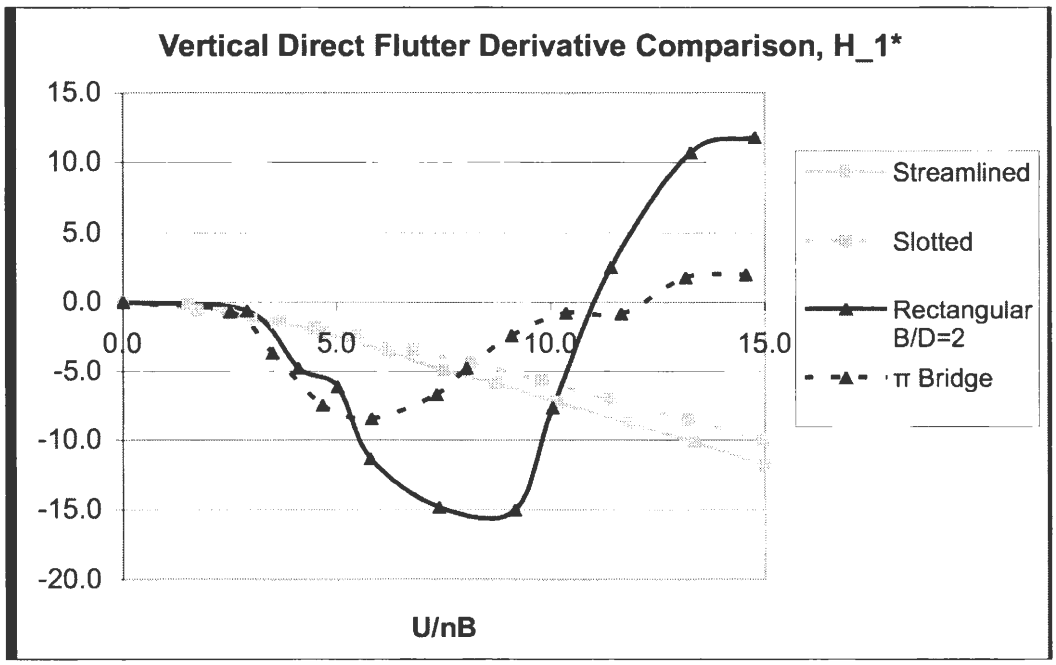

Figure 28a. Vertical direct flutter derivative, H_1*, comparison for all models tested

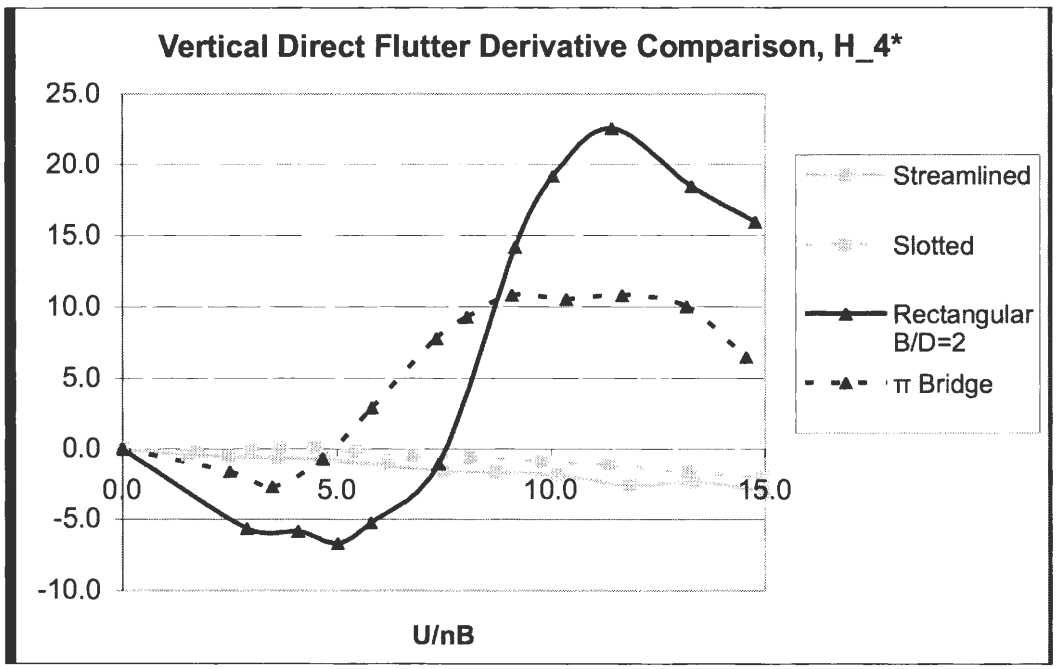

Figure 28b. Vertical direct flutter derivative, H_4*, comparison for all models tested

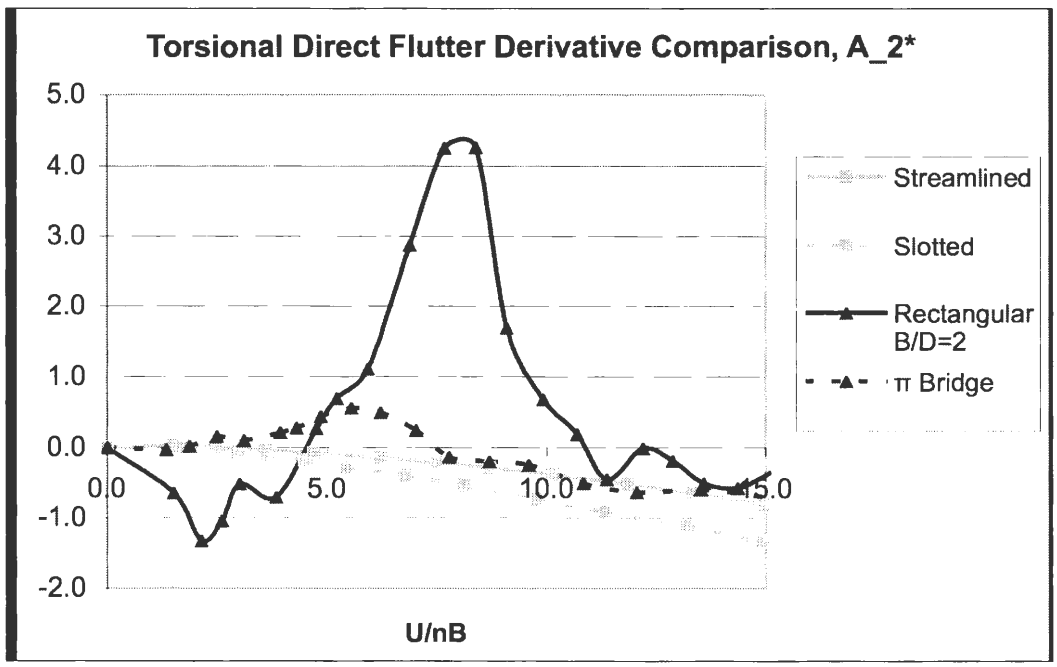

Figure 28c. Torsional direct flutter derivative, A_2*, comparison for all models tested

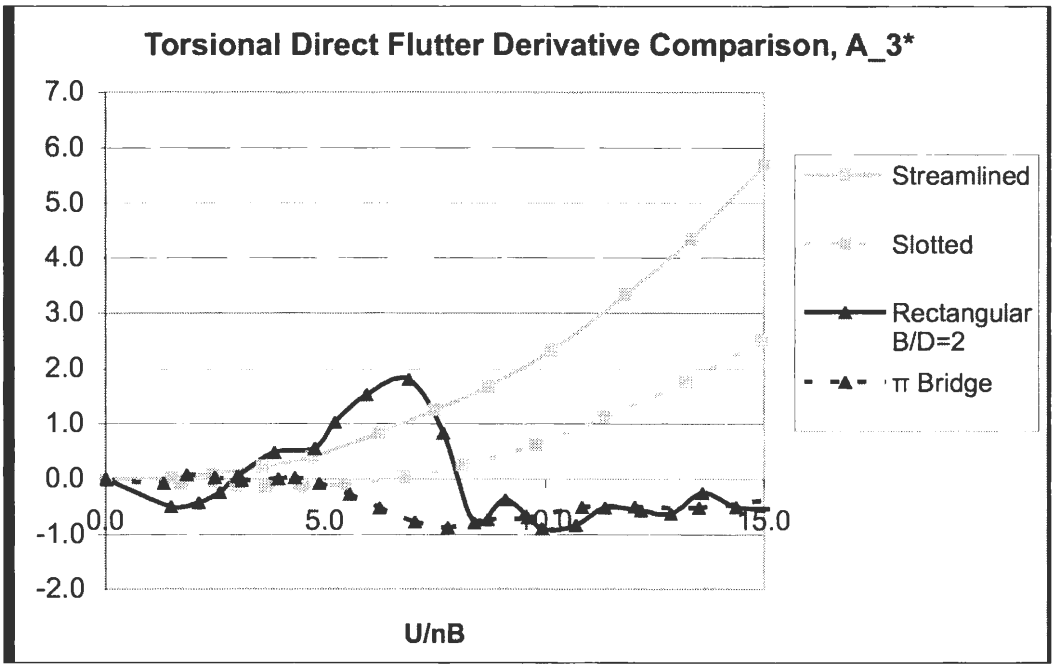

Figure 28d. Torsional direct flutter derivative, A_3*, comparison for all models tested

For all direct flutter derivatives, except for A_3^*, the streamlined box girder and slotted-streamlined box girder showed characteristics of stable bridge decks. The flutter derivatives H_1^*, H_4^*, and A_2^* for the slotted-streamlined and streamlined bridge decks go to negative values throughout the reduced velocity range. The rectangular (B/D=2) bluff-body bridge deck would be considered the most unstable configuration due to very high positive values for the majority of the flutter derivatives. The Π-shaped bridge also exhibited signs of an unstable bridge deck. The Π-shaped bridge was stable in the torsional-DOF for most of the reduced velocity range. The unstable bridge decks, the Π-shaped bridge and the rectangular box girder bridge, showed signs of vertical stability at lower velocities, vertical instability at higher velocities, and torsional instability at the middle range of reduced velocities.

During testing of the Π-shaped bridge, irregular disturbances were noticed within the displacement time histories in the upper half of the reduced velocity ranges. These disturbances added to the instability of the model, causing constant changes in the aerodynamic damping. Figure (29) shows a sample displacement time history of the vertical-DOF and torsional-DOF from the Π-shaped bridge. Originally this characteristic oscillatory motion was thought to have occurred from model flexibility or from model mounting clamp sloppiness. Alterations were performed on the model to increase stiffness in the mounting clamps. It was concluded that the stiffness of the model was not an issue. This phenomenon was believed to have occurred due to either vortex shedding from the upper and lower surfaces at different rates, or flow separation on the lower surface with attached flow on the upper surface. These ideas were developed from flow theories over flat plates and bluff-bodies. Flow over flat plates remains attached at low angles of attack, while flow over bluff-bodies separates from the surface. The lower surface of the Π-shaped bridge represents a more bluff shape than the upper surface.

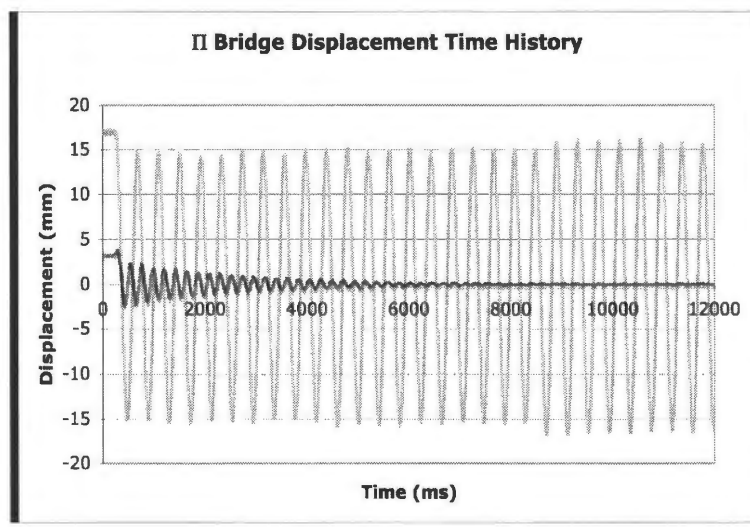

Figure 29. Π-shaped bridge two-DOF displacement time history

As discussed in Chapter 3, part of this study involved a comparison of the ISU WiST Lab flutter derivative results with those of Matsumoto and Sato. A major issue when comparing data of this nature is verifying that the data is scaled correctly. Incorrect scaling could result from a number of sources, but the particular source for scaling issues with this comparison originated in the parameters used to derive the flutter derivative equations. One such parameter was the bridge deck width. The method used in the ISU WiST Lab uses the full width in the flutter derivative equations as well as in the reduced velocity equation, while the data of Matsumoto being compared to used the half-width. The flutter derivative comparisons are shown in Figures (30a,b,c,d) and (31a,b,c,d).

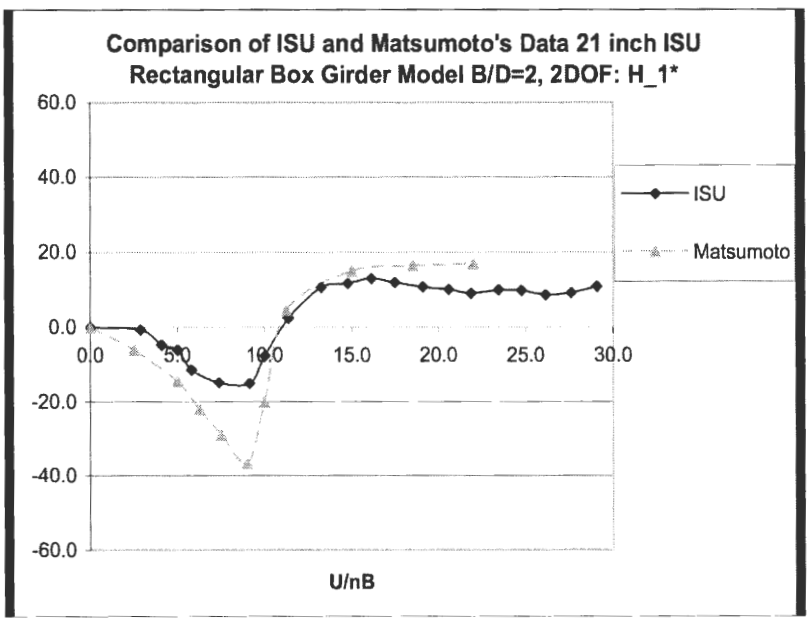

Figure 30a. Vertical flutter derivative, H_1^*, comparison (Matsumoto / ISU) for rectangular box girder, B/D=2

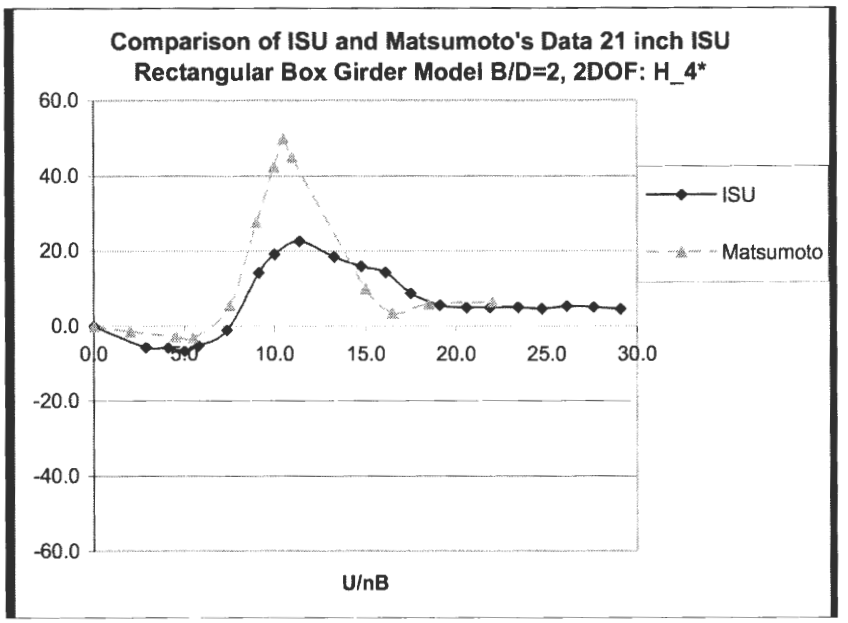

Figure 30b. Vertical flutter derivative, H_4^*, comparison (Matsumoto / ISU) for rectangular box girder, B/D=2

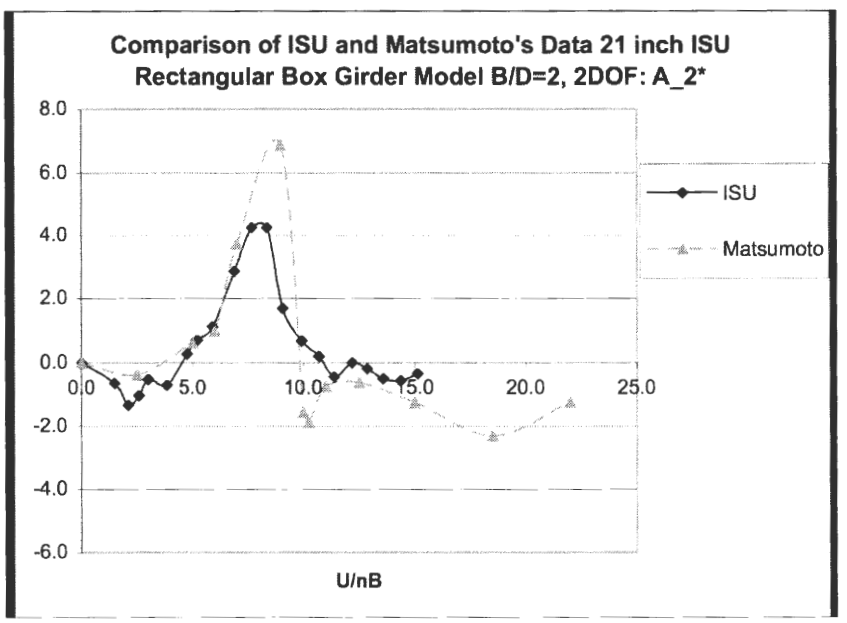

Figure 30c. Torsional flutter derivative, A_2^*, comparison (Matsumoto / ISU) for rectangular box girder, B/D=2

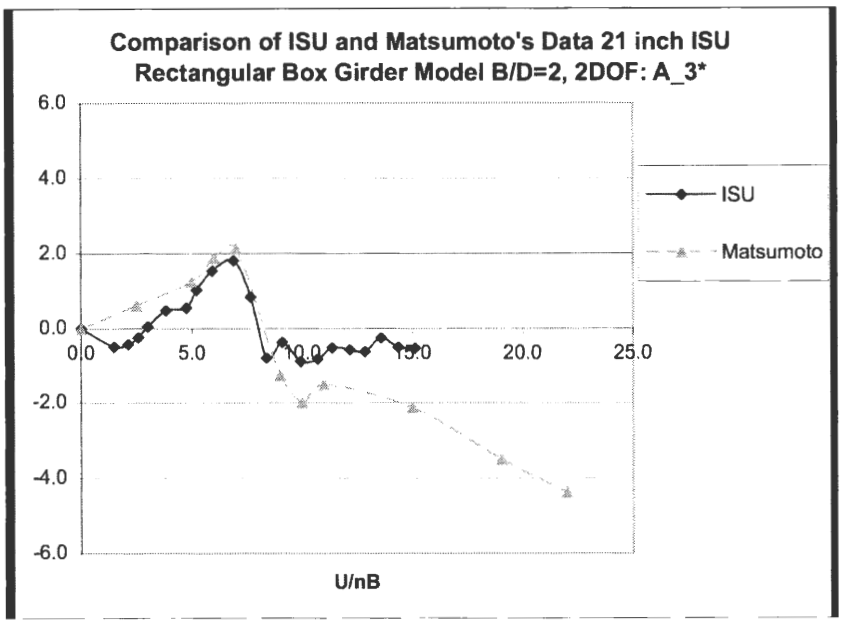

Figure 30d. Torsional flutter derivative, A_3^*, comparison (Matsumoto / ISU) for rectangular box girder, B/D=2

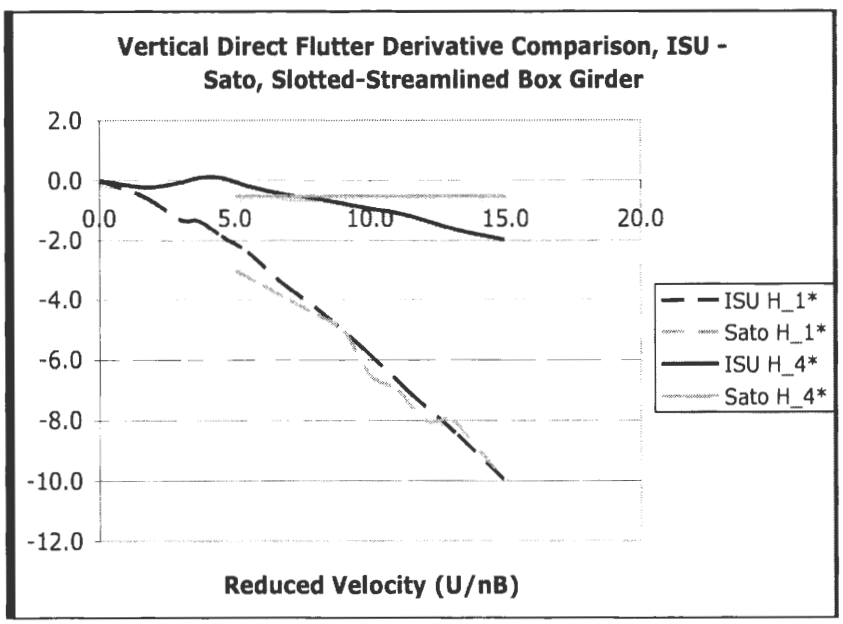

Figure 31a. Vertical direct flutter derivative comparison (ISU / Sato) for slotted-streamlined box girder

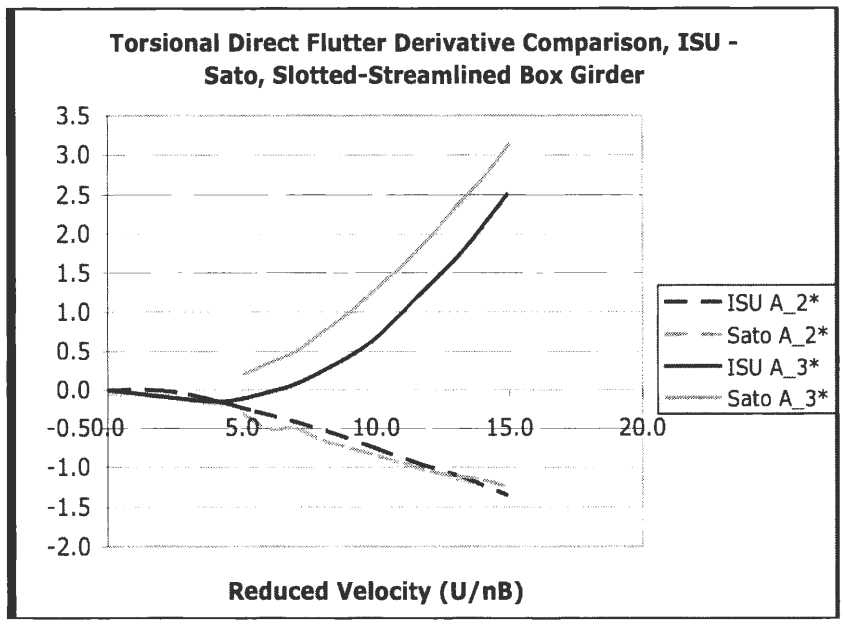

Figure 31b. Torsional direct flutter derivative comparison (ISU / Sato) for slotted-streamlined box girder

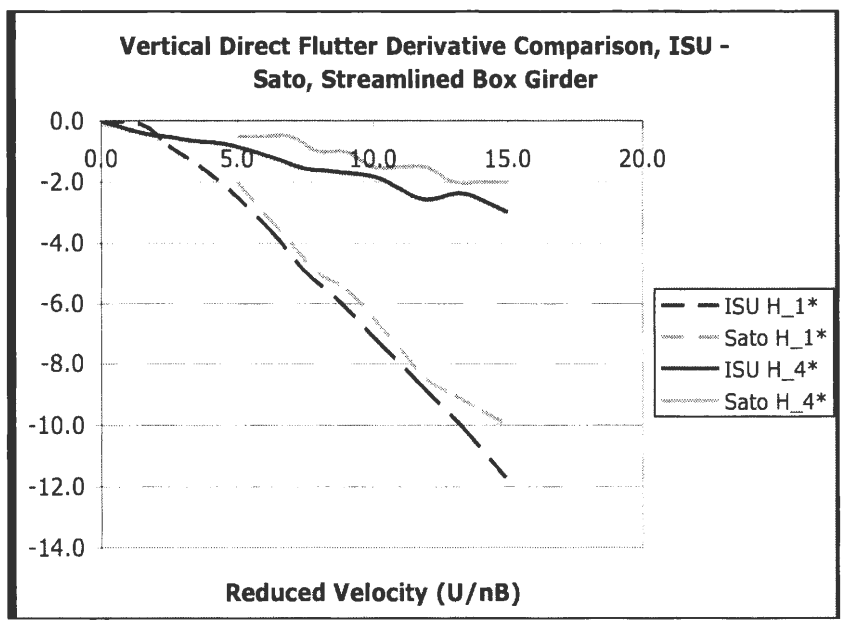

Figure 31c. Vertical direct flutter derivative comparison (ISU / Sato) for streamlined box girder

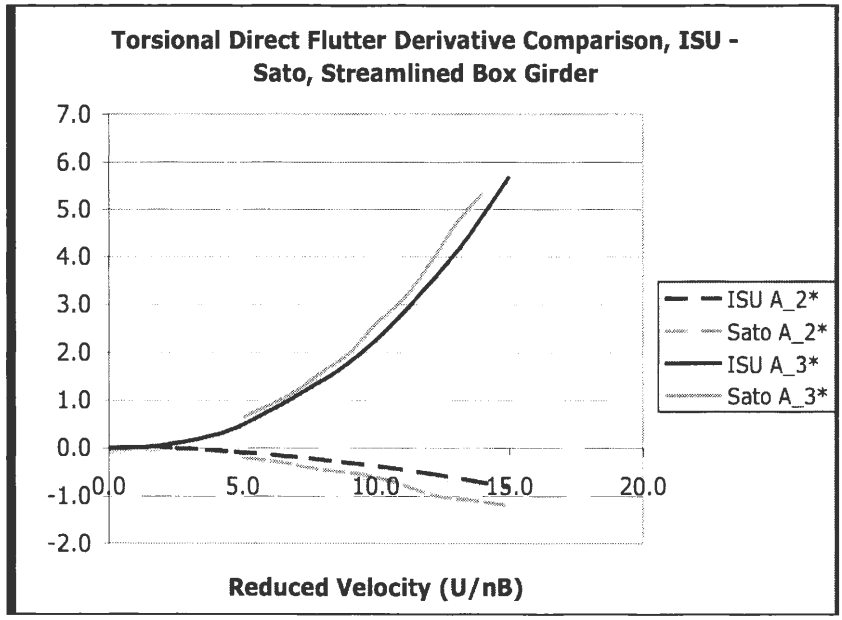

Figure 31d. Torsional direct flutter derivative comparison (ISU / Sato) for streamlined box girder

As can be seen from the previous charts, the flutter derivatives obtained in the ISU WiST Lab have similar values to those from Matsumoto (for the rectangular box girder, B/D=2) and Sato (for the streamlined and slotted-streamlined box girders). The trends appear alike in all plots with peaks, slopes, and zero-crossings occurring in comparable locations. Performing this comparison helped to establish increasing confidence in the data obtained in the ISU WiST Lab.

Both Matsumoto and Sato used a forced-oscillation setup to extract the flutter derivatives from their corresponding models. The closeness of the comparison between the ISU WiST Lab data and that of Matsumoto and Sato helps to prove the consistency between the free-vibration and forced-oscillation methods. Great attention was placed on using similar initial conditions to those of Matsumoto and Sato to produce comparable results. When comparing the rectangular box girder flutter derivatives it was noticed that Matsumoto

used an initial vertical amplitude of approximately 2mm and a torsional amplitude of 2 degrees. The differences in the vertical amplitude could have been the cause of any inconsistencies during the comparison of the rectangular box girder. Bluff-body bridge decks are more prone to changes in resulting flutter derivatives when these inconsistencies exist between the initial amplitude of subsequent tests.

Chapter 5: Summary and Conclusions - Recommendations and Future Research

5.1 Summary and Conclusions

The main focus of this research project was to test the robustness and improve the efficiency of the free-vibration flutter derivative extraction technique using the ILS method at the ISU WiST Lab. The robustness and efficiency of the technique was demonstrated by conducting tests on multiple models of different shapes and aerodynamic characteristics. The contributions to this methodology included exploring alternate model building methods that sometimes required pressure taps to be an integral part of the model, streamlining of the data analysis procedure by making the analysis software more robust and user-friendly, and making the magnetic system for applying the initial conditions in the elastic suspension system more workable. As a final step for checking correct system operation, the output data was verified through rigorous comparisons. Many characteristics of the suspension system and free-vibration analysis were studied to help establish testing standards. These standards were deemed important during data comparison.

The model development helped to provide insight for future testing with the suspension system as well as with various other test apparatuses in the ISU WiST Lab. Many issues arose during the initial stages of CAD / Rapid Prototyping (RP) model building, but these were confronted and addressed to prevent future recurrences with similar designs. The establishment of a standard for CAD / RP model construction is important for future research, particularly those requiring pressure taps incorporated into thin-walled model components.

Models that were predicted prior to testing as stable or unstable due to the geometric configurations showed as such after analysis. This provided a qualitative evaluation of the free-vibration flutter analysis method used in the ISU WiST Lab. The Π-shaped bridge and rectangular box girder bridge were initially thought of as unstable designs, and were proven to be unstable after flutter analysis. The quantitative analysis involved comparing output data from this research to data from Matsumoto [22] and Sato [23]. The comparison of Matsumoto's and Sato's data to the ISU WiST Lab data provided a platform for developing testing standards used for comparing data. Comparison plots revealed that the current free-vibration flutter analysis yielded flutter derivatives for the Π-shaped bridge and rectangular box girder bridge that had the same trend as obtained by others but somewhat different magnitudes. The comparisons of the streamlined box girder and the slotted-streamlined box girder results with those of Sato [23] were almost perfect.

Redevelopment of the ILS System ID software helped to streamline the data analysis processes. The software was made more efficient and user-friendly to help simplify the extraction of flutter derivatives of multiple bridge deck models. This aided in the ability to analyze and re-analyze data with minimal code alteration and downtime.

5.2 Recommendations

The recommendations pertain to further research with the use of the free-vibration system under development in the ISU WiST Lab. These recommendations focus on improvements to the components of the free-vibration suspension system and further refinement of the CAD/RP model building technique. The suspension system in use for this research was originally a prototype. Since the system provided reasonable data, no major

improvements were considered. If many other structures are to be analyzed then the system must be made more robust to provide consistent and trouble-free operation. With reference to Figure (3) in Chapter 2, the horizontal rods should be replaced by a pair of horizontal rods on each side of the section model. This would reduce the stiffness and strength requirements for the section models. Currently, large amounts of torque are transferred through the model from the initial condition apparatus. This causes irregular motion upon model release as well as occasional binding in the linear air bearings. Using a pair of rods would eliminate the torque and therefore reduce structural requirements of the model and further streamline testing.

If more complex section models are needed for future research, and these models are designed and built using the CAD / RP approach then a higher quality RP system should be used. The RP system used to build the Π-shaped Bridge and also used for preliminary design and construction of the Tacoma Narrows Bridge was too limited in capabilities. The resolution of the machine did not allow for exact scaling when individual bridge parts became very small. This could also be critical when incorporating pressure taps in these miniature parts. Higher resolution machines are available. These machines would carry higher operational costs, but higher quality models would be worth the expense.

5.3 Future Research

During the course of this research, four bridge decks were considered for flutter analysis. The fifth bridge, the Tacoma Narrows Bridge, could be analyzed to allow further verification of the ISU WiST Lab free-vibration flutter analysis system. Much data is available for the Tacoma Narrows Bridge for an additional comparative analysis. The model

currently in development could be utilized as a section model for both the free-vibration system and the forced-oscillation system.

Additional work pertaining to the Bill James Wind Tunnel suspension system includes final construction and testing of a forced-oscillation system. The forced-oscillation system currently under development is shown in Figure (4) and Figure (5) in Chapter 2. Currently, plans are under way to use this system to perform a benchmark study in the ISU WiST Lab using the same group of five models used for the free-vibration flutter analysis. These plans also include a collaborative US-Japan flutter derivative benchmark study. To perform the above-mentioned studies, some of the models would need to be reconstructed with the addition of pressure taps. The models would be tested in the same wind tunnel, same test section, and using the same suspension system as the free-vibration system. This would eliminate many scaling parameters as well as other differences between the ISU WiST Lab configuration and sources for comparison data. This would also provide a direct comparison of the same bridge deck configurations using a completely different analysis method. The above would allow for a verification of both analysis techniques utilized in the ISU WiST Lab for flutter research.

References

[1] Cochran, L.S. "Wind Effects on Lowrise Buildings, Proceedings of the Second National Conference on Wind Engineering, Commemorative Volume to Honour Professor Prem Krishna." Indian Society of Wind Engineering Vol.1 (2004): 79-99.

[2] Tacoma Narrows Bridge Collection, University of Washington Libraries Digital Collections. http://content.lib.washington.edu/farquharsonweb/

[3] Gan Chowdhury, Arindam and Partha P. Sarkar. "A new technique for identification of eighteen flutter derivatives using a three-degree-of-freedom section model." Engineering Structures Vol. 25 (2003): 1763-1772.

[4] Braun, A.L. and A.M. Awruch. "Numerical Simulation of the wind action on a long-span bridge deck." Journal of the Brazilian Society of Mechanical Sciences and Engineering Vol. 25 (2003).

[5] Larsen, Allen and Jens H. Walther. "Discrete vortex simulation of flow around five generic bridge deck sections." Journal of Wind Engineering and Industrial Aerodynamics Vol. 77 and 78 (1998): 591-602.

[6] Gu, Ming and Xian-Rong Qin. "Direct identification of flutter derivatives and aerodynamic admittances of bridge decks." Engineering Structures Vol. 26 (2004): 2161-2172.

[7] Sarkar, P.P., A.G. Chowdhury, and T.B. Gardner. "A novel elastic suspension system for wind tunnel section model studies." Journal of Wind Engineering and Industrial Aerodynamics Vol. 92 (2004): 23-40.

[8] Sarkar, P.P. "New-identification methods applied to the response of flexible bridges to wind." PhD thesis. Baltimore, MD: The Johns Hopkins University (1992).

[9] Sarkar, P.P., N.P. Jones, R.H. Scanlan. "System identification for estimation of flutter derivatives." Journal of Wind Engineering and Industrial Aerodynamics Vol. 41-44 (1992): 1243-54.

[10] Sarkar, P.P., N.P. Jones, R.H. Scanlan. "Identification of aeroelastic parameters of flexible bridges." Journal of Engineering Mechanics ASCE Vol. 120(8) (1994): 1718-42.

[11] Imai, H., C.B. Yun, O. Maruyama, and M. Shinozuka. "Fundamentals of system identification in structural dynamics." Prob Eng Mech Vol. 4 (1989): 162-73.

[12] Hsia, T.C. "On least squares algorithms for system parameter identification." IEEE Trans Autom Contr Vol. 21(1) (1976): 104-8.

[13] Yamada, H. and H. Ichikawa. "Measurement of aerodynamic parameters by extended Kalman filter algorithm." Journal of Wind Engineering and Industrial Aerodynamics Vol. 42 (1992): 1255-63.

[14] Diana, G., F. Cheli, and F. Resta. "Time domain aeroelastic force identification on bridge decks." In: Proce 9th Int Conf Wind Eng, New Delhi, India. Wiley Easter Ltd.; (1995): 938-49.

[15] Iwamoto, M., Y. Fujino. "Identification of flutter derivatives of bridge deck from free vibration data." Journal of Wind Engineering and Industrial Aerodynamics Vol. 54/55 (1995): 55-63.

[16] Jones, N.P., T. Shi, J.H. Ellis, and R.H. Scanlan. "System-identification procedure for system and input parameters in ambient vibration surveys." Journal of Wind Engineering and Industrial Aerodynamics Vol. 54/55 (1995): 91-9.

[17] Jakobsen, J.B., E. Hjorth-Hansen. "Determination of the aerodynamic derivatives by a system identification method." Journal of Wind Engineering and Industrial Aerodynamics Vol. 57 (1995): 295-305.

[18] Brownjohn, J.M.W., J.B. Jakobsen. "Strategies for aeroelastic parameter identification from bridge deck free vibration data." Journal of Wind Engineering and Industrial Aerodynamics Vol. 89 (2001): 1113-36.

[19] Gu, M, R. Zhang, and H. Xiang. "Identification of flutter derivatives of bridge decks." Journal of Wind Engineering and Industrial Aerodynamics Vol. 84 (2000): 151-62.

[20] Zhu, L.D., Y.L. Xu, F. Zhang, and H.F. Xiang. "Tsing Ma bridge deck under skew winds. Part II: Flutter derivatives." Journal of Wind Engineering and Industrial Aerodynamics Vol. 90 (2002): 807-37.

[21] Chowdhury, Arindam Gan and Partha P. Sarkar. "Identification of eighteen flutter derivatives of an airfoil and a bridge deck." Wind and Structures Vol. 7(3) (2004): 187-202.

[22] Matsumoto, M. "Aerodynamic Damping of Prisms." Journal of Wind Engineering and Industrial Aerodynamics Vol. 59 (1996): 159-175.

[23] Sato, Hiroshi, Jun Murakoshi, and Koichiro Fumoto. "Benchmark study on flutter derivatives." Measurement at PWRI, Japan. *Draft*

Acknowledgments

I regard my experiences with the Iowa State University Wind Simulation and Testing Laboratory as the "stepping stone" to propel myself to the place in life I envisioned when my journey at ISU began. I want to express my gratitude to my major professor Dr. Partha P. Sarkar for providing the numerous, valuable learning experiences during my undergraduate and graduate work. Had it not been for Dr. Sarkar's strong determination to convince me to continue my education into a graduate degree, I would not be where I stand today. His ambition reminds me that no matter how impossible a goal may seem there is always a way to reach it.

I would also like to thank my committee members, Dr. Fred Haan and Dr. Mani Mina for taking time out of their busy schedules to evaluate my performance. Dr. Haan has been a great inspiration as a researcher and has provided a significant amount of knowledge on overcoming obstacles with the ingredients of inquisitiveness, determination, and elbow grease.

I want to also thank all of those who have supported me throughout my years as an undergraduate and graduate student at Iowa State University. These people include Bill Rickard, Gayle Fay, Dee Pfeiffer, and my fellow graduate students and coworkers. Your assistance is appreciated and your friendship will always be remembered.

Last, but definitely not least, I would like to thank my parents and siblings. They have stood behind me throughout my successes and failures, always offering words of encouragement to push onward. I realize that the start of my journey will always be home, where I learned the basics to get me through life.